

Caveolin targeting to late endosome/lysosomal membranes is induced by perturbations of lysosomal pH and cholesterol content

Dorothy I. Mundy^a, Wei Ping Li^b, Katherine Luby-Phelps^b, and Richard G. W. Anderson^b

^aDepartment of Internal Medicine-Touchstone Diabetes Center and ^bDepartment of Cell Biology, University of Texas Southwestern Medical Center, Dallas, TX 75390

ABSTRACT Caveolin-1 is an integral membrane protein of plasma membrane caveolae. Here we report that caveolin-1 collects at the cytosolic surface of lysosomal membranes when cells are serum starved. This is due to an elevation of the intralysosomal pH, since ionophores and proton pump inhibitors that dissipate the lysosomal pH gradient also trapped caveolin-1 on late endosome/lysosomes. Accumulation is both saturable and reversible. At least a portion of the caveolin-1 goes to the plasma membrane upon reversal. Several studies suggest that caveolin-1 is involved in cholesterol transport within the cell. Strikingly, we find that blocking cholesterol export from lysosomes with progesterone or U18666A or treating cells with low concentrations of cyclodextrin also caused caveolin-1 to accumulate on late endosome/lysosomal membranes. Under these conditions, however, live-cell imaging shows caveolae actively docking with lysosomes, suggesting that these structures might be involved in delivering caveolin-1. Targeting of caveolin-1 to late endosome/lysosomes is not observed normally, and the degradation rate of caveolin-1 is not altered by any of these conditions, indicating that caveolin-1 accumulation is not a consequence of blocked degradation. We conclude that caveolin-1 normally traffics to and from the cytoplasmic surface of lysosomes during intracellular cholesterol trafficking.

Monitoring Editor
Howard Riezman
University of Geneva

Received: Jul 6, 2011
Revised: Oct 31, 2011
Accepted: Jan 5, 2012

INTRODUCTION

Caveolae are 60- to 100-nm, omega-shaped membrane domains rich in cholesterol and sphingolipids and are found on the plasma membrane of most cells. Caveolin-1 is the marker protein commonly used to identify this domain (Rothberg *et al.*, 1992). Caveolin-1 is a 178-amino acid, integral membrane protein that forms a hairpin within the lipid bilayer with both the C- and the N-terminus facing the cytoplasm (Dupree *et al.*, 1993). Caveolin-1 is required to form invaginated caveolae since ultrastructural examination of tissues from caveolin-1^{-/-} animals showed that omega-shaped structures

were completely absent (Drab *et al.*, 2001). Recent studies have implicated polymerase I and transcript release factor (PTRF)/cavin-1 as another putative coat protein selectively associated with mature caveolae at the plasma membrane (Vinten *et al.*, 2001; Voldstedlund *et al.*, 2001; Aboulaich *et al.*, 2004; Hill *et al.*, 2008; Liu and Pilch, 2008), and other cavin family members may also play a role in caveolae structure or function (McMahon *et al.*, 2009; Verma *et al.*, 2010).

Unlike in clathrin-mediated endocytosis, the caveolin coat remains attached to the caveolin-coated vesicle and can be used as a marker to follow the intracellular trafficking of this membrane domain. Live-cell imaging has confirmed and extended our understanding of the dynamic behavior of caveolae. Kirkham *et al.* (2005) showed that in mouse embryo fibroblasts ~2% of the caveolin-coated cell surface is internalized per minute. That rate can be doubled by treatment with the phosphatase inhibitor okadaic acid (Parton *et al.*, 1994) or by the glycosphingolipid lactosyl ceramide (Sharma *et al.*, 2004). Once believed to be relatively immobile structures engaged in transendothelial transport of blood-borne molecules (Simionescu, 1983), studies using caveolin-1-GFP showed that there are at least three distinct types of caveolae traffic (Mundy *et al.*, 2002). Type I

This article was published online ahead of print in MBoC in Press (<http://www.molbiolcell.org/cgi/doi/10.1091/mbc.E11-07-0598>) on January 11, 2012.

Address correspondence to: Dorothy I. Mundy (dorothy.mundy@utsouthwestern.edu).

Abbreviations used: FITC/RH-dex, FITC rhodamine dextran; LAMP, lysosomal membrane-associated membrane protein-1; LE, late endosomes; MβCD, methyl-β-cyclodextrin; OG-dex, Oregon green dextran.

© 2012 Mundy *et al.* This article is distributed by The American Society for Cell Biology under license from the author(s). Two months after publication it is available to the public under an Attribution-Noncommercial-Share Alike 3.0 Unported Creative Commons License (<http://creativecommons.org/licenses/by-nc-sa/3.0>).

"ASCB®," "The American Society for Cell Biology®," and "Molecular Biology of the Cell®" are registered trademarks of The American Society of Cell Biology.

caveolae detach from the membrane to form cavicles (caveolin-coated vesicles) that travel on microtubules deep into the cell interior. Cavicles may carry cargo to special endosomes that are pH neutral called caveosomes (Pelkmans *et al.*, 2001), but they may also deliver molecules to other destinations. Type II caveolae, which are the most numerous type in tissue culture cells, appear to be in equilibrium between individual and multicaveolar assemblies at the cell surface. The individual caveolae in total internal reflection fluorescence images appear to undergo short-range fission and fusion interactions, whereas the larger, multicaveolar assemblies remain open to the extracellular space (Pelkmans and Zerial, 2005). Recent studies extended these findings and suggest that 85% of the caveolae are dynamic over a period of 10 min (Boucrot *et al.*, 2011). Actin controls much of this type II traffic. Localized dissolution of the actin cytoskeleton seems to be required for the switch from the plasma membrane-localized dynamics of caveolae to a committed internalization step that is microtubule dependent. The final type of caveolar traffic (type III) involves formation of long, caveolin-1-positive, highly dynamic tubules that extend deep into the cell interior. No function has been identified for these tubules, although their formation appears to be stimulated by Shiga toxin (Hansen *et al.*, 2009). Recent studies suggest that both Rab8 and PTRF/cavin1 are important in regulating their formation (Verma *et al.*, 2010).

Cholesterol is central to both the structure and function of caveolae. Studies with a photoactivatable form of cholesterol showed that caveolin is a major cholesterol-interacting protein (Thiele *et al.*, 2000). Moreover, cholesterol is considerably more abundant in caveolae than in the surrounding plasma membrane (Simionescu, 1983), suggesting that caveolae have a special capacity to sequester large amounts of cholesterol. When cholesterol is depleted from cells, caveolae that are visible as flask-shaped invaginations by electron microscopy (EM) collapse into the plane of the membrane (Rothberg *et al.*, 1992), and caveolin is free to diffuse away. Normally single caveolae do not readily exchange subunits but remain as intact entities on the cell surface. Only when cholesterol is depleted does exchange of individual caveolin molecules between caveolae occur (Tagawa *et al.*, 2005). The biogenesis of caveolae in the Golgi apparatus also requires cholesterol (Parton *et al.*, 2006), and cholesterol levels modulate caveolin trafficking through this organelle to the cell surface (Pol *et al.*, 2005). Cholesterol depletion has been used extensively as an inhibitor of caveolin/caveolae function (for reviews see Williams and Lisanti, 2004; Pelkmans, 2005; Cheng *et al.*, 2006a; Parton and Simons, 2007). Caveolin-1 binds both cholesterol (Murata *et al.*, 1995) and long-chain unsaturated fatty acids (Trigatti *et al.*, 1999), which raises the possibility that caveolin-1 is part of a cholesterol/fatty acid supply system. Indeed, there is mounting evidence for a requirement for caveolin in regulating cholesterol homeostasis and in intracellular cholesterol trafficking (Ikonen and Parton, 2000; Martin and Parton, 2005; Frank *et al.*, 2006). How caveolin with its prominent hydrophobic characteristics ferries cholesterol through the hydrophilic environment of the cytoplasm and delivers it to its final destination is not known.

Here we describe a new behavior of caveolin-1, one that might be related to its role in cholesterol transport or homeostasis. We show that when cells are serum starved caveolin-1 accumulates on the cytoplasmic surface of the membranes that surround late endosomes and lysosomes (LE/lysosomes). Caveolin-1 also accumulates on LE/lysosome membranes when cholesterol homeostasis is perturbed either by low concentrations of cyclodextrin or when the egress of lysosomal cholesterol is blocked using progesterone or U18666A (Butler *et al.*, 1992; Cenedella, 2009). A recent article suggested that caveolin translocates to lysosomes primarily to be de-

graded (Hayer *et al.*, 2010). Although this is undoubtedly true when tagged caveolins are transiently overexpressed or, as Hill *et al.*, (2008) reported, when PTRF/cavin1 is knocked down and caveolin enters the cell via the bulk endocytic pathway, this is not the case here. We show that neither serum starvation nor U18666A changes the turnover rate of endogenous caveolin or caveolin-1-green fluorescent protein (GFP) that is stably expressed in cells. Cavicles normally shuttle between membranes without a loss of domain identity, and when they accumulate on LE/lysosomes after progesterone or U18666A treatment they appear to retain their identity as punctate structures. In contrast, when lysosomal pH is high the caveolin that is associated with LE/lysosomes is evenly distributed over the membrane surface, suggesting that the structure of the cavicle/caveolae is significantly different. In addition, when the association of caveolin-1 with LE/lysosomes is reversed after serum starvation caveolin-1 leaves by a process that appears not to involve cavicles and is not inhibited by genistein, whereas this inhibitor blocks trafficking to the LE/lysosome.

RESULTS

Redistribution of caveolin to LE/lysosomes

We used a CHO cell line that stably expresses caveolin-1-GFP to study the intracellular trafficking of caveolin. Previously we showed that caveolin-1-GFP behaves like endogenous caveolin and that the trafficking of caveolin requires both the actin cytoskeleton and microtubules (Mundy *et al.*, 2002). These earlier studies were all done in normal growth medium containing fetal calf serum. Under these conditions, caveolin is primarily located at the plasma membrane, on several internal membrane structures and on cavicles (Figure 1A). In contrast, when cells are treated overnight in the absence of serum, caveolin-1 colocalizes with LysoTracker-positive vesicles (Figure 1, D and E). LysoTracker is a dye that accumulates in the LE/lysosomes in live cells (Figure 1, B and E; Liu *et al.*, 1999; Mesa *et al.*, 2001; Li *et al.*, 2004). Quantification of the fluorescence on these structures demonstrated that $15.7 \pm 2\%$ (SEM) (see *Materials and Methods*) of the total caveolin is redistributed to LE/lysosomes, indicating that significant amounts of caveolin-1 are still associated with the plasma membrane (arrowheads in Figure 1G). The LysoTracker- and caveolin-positive structures generally cluster in the perinuclear area of the cell and display both saltatory movements and rapid translocation throughout the cell (Figure 1G and Supplemental Video S1). Live-cell imaging shows that LysoTracker and caveolin-1-GFP move together, providing strong evidence that they are on the same structure (Figure 1H and Supplemental Video S2). Caveolin-1 is not associated with LysoTracker positive-vesicles in control cells (Figure 1, B and C). Moreover, caveolin-1-positive vesicles move independently of LysoTracker-positive vesicles in cells maintained in growth medium (Figure 1I and Supplemental Video S3). Similar results were obtained using fluorescently tagged dextrans to visualize LE/lysosomes.

To confirm that caveolin-1-GFP was associated with LE/lysosomes in serum-starved cells, we used EM immunogold labeling. Figure 2A shows that serum-deprived cells contain LE/lysosomes (Ly) that are extensively labeled with an anti-GFP immunoglobulin G (IgG; 10-nm gold). We quantified the gold labeling on 50 LE/lysosomes from either control cells maintained in growth medium (growth, Figure 2B) or cells grown overnight in serum-free media (starve). As shown in the bar graph, we found 430 gold particles associated with LE/lysosomes in serum-starved cells but only nine gold particles on the same number of LE/lysosomes in control cells. Besides demonstrating that caveolin-1-GFP is present on LE/lysosomes, the labeling pattern suggested that the caveolin-1-GFP is

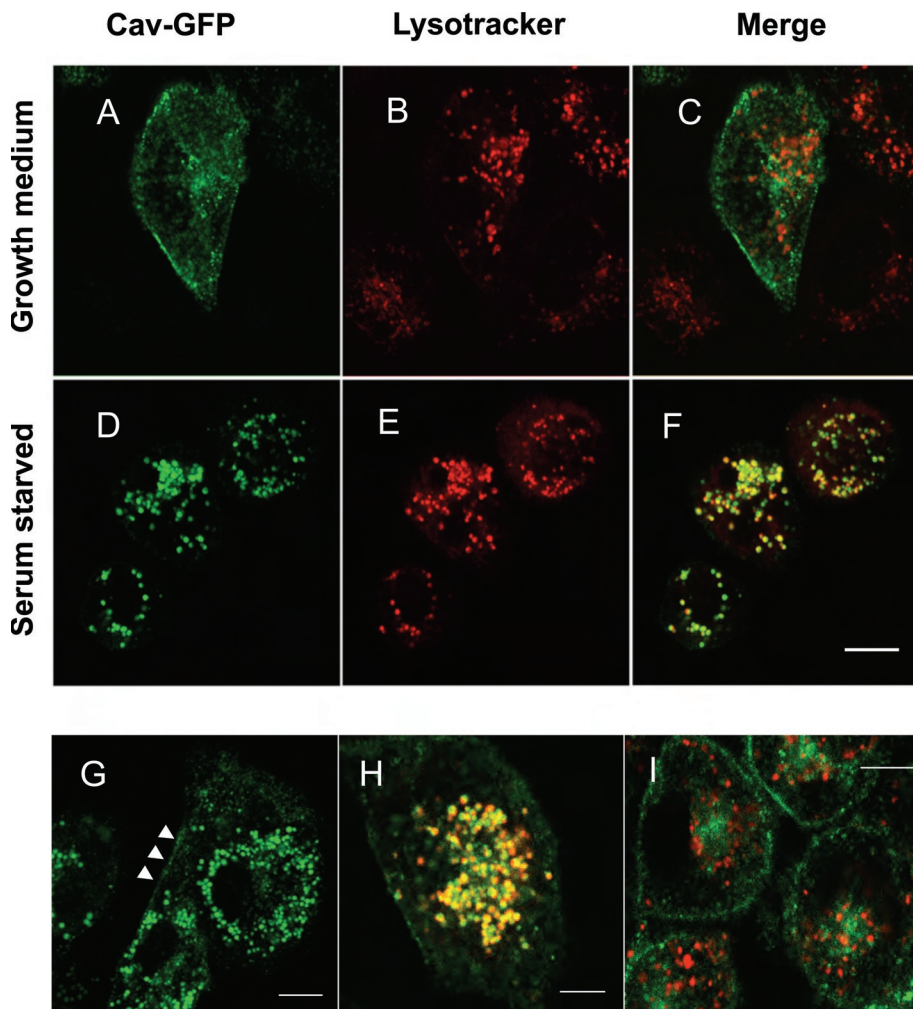


FIGURE 1: Caveolin is translocated to LE/lysosomes in starved cells. CHO cells stably transfected with caveolin-1-GFP were plated onto glass-bottomed dishes in growth medium 2 d before the cells were to be imaged. The next day the medium was replaced with either fresh growth medium (A–C, I) or serum-free medium (D–H) for 16 h. Before imaging the cells were labeled with 50 nM LysoTracker for 30 min. In growth medium caveolin is not associated with the LE/lysosomal compartments (A–C). However, caveolin redistributes to preexisting LE/lysosomal structures when cells are starved (D–F). Some caveolin remains at the plasma membrane in starved cells (G, arrowheads). Greater than 95% of the cells show this redistribution, and the experiment was repeated more than 20 times. LE/lysosomes positive for caveolin-1-GFP in starved cells showed both localized and long-range movements (G, and Supplemental Video S1). Supplemental Video S2 (H) shows that structures labeled with LysoTracker (red) were labeled with caveolin-1-GFP (green) and moved together. In control cells (I), LysoTracker-labeled structures moved independently of caveolin-1-GFP labeled structures (see Supplemental Video S3). Scale bar, A–G, I, 10 μ m; H, 5 μ m.

primarily on the external surface of the LE/lysosome and does not enter the lumen, where it might be degraded. Of the 430 gold particles found on LE/lysosomes in starved cells, 369 were within 20 nm of the outer surface, suggesting that caveolin-1-GFP decorates the limiting membrane of LE/lysosomes.

Importantly, endogenous caveolin also became associated with LE/lysosomes in response to serum deprivation using anti-caveolin-1 IgG and immuno-EM (Figure 2, C–E). Caveolin-1 has a normal distribution in CHO cells maintained in growth medium, and is primarily located at the plasma membrane in caveolae, with no apparent labeling of lysosomes (Figure 2, C and D). After serum starvation, however, large, single-membrane bound structures with the typical morphology of LE/lysosomes became decorated with en-

dogenous caveolin-1 (Figure 2E). The number of gold particles associated with caveolae, plasma membrane (PM), and lysosomes is quantified in the table (Figure 2). In serum-starved cells there was an increase in the number of gold particles associated with LE/lysosomes and a concomitant decrease in the number of gold particles associated with caveolae both in the stable cell line and when we examined endogenous caveolin in untransfected cells. EM analyses show that there are no obvious ultrastructural differences between cells that are maintained in growth medium or those incubated in serum-free medium overnight (Supplemental Figure S1, A–D) and that serum starvation does not induce autophagy (Supplemental Figure S1E). Both the EM and the LysoTracker studies showed that there were no significant differences in either the size or number of lysosome-like structures between the serum-starved cells and the cells maintained in growth medium (Figure 1, compare B and E). There are also no obvious differences between the cells stably expressing caveolin-1-GFP and the parental CHO cell line (Supplemental Figure S1, compare A and C with B and D). These data establish that endogenous caveolin traffics to lysosomes when cells are starved and that our observations in transfected cells are not an artifact of the exogenous expression of caveolin-1-GFP.

To test whether the caveolin-1 redistribution to LE/lysosomes was a general property of caveolin behavior, we examined caveolin trafficking in other cell types, including SV589 fibroblasts. Lysosomal membrane-associated protein-1 (LAMP-1) is a type 1 transmembrane glycoprotein that is a well-accepted LE/lysosome membrane marker (Chen *et al.*, 1985; Rohrer *et al.*, 1996). Using antibodies to human LAMP-1, we were able to confirm that the structures labeled in live cells with caveolin were LE/lysosomes. Supplemental Figure S2 shows the colocalization of caveolin-1-GFP with LAMP-1-labeled structures when cells are serum starved (D–F) and no labeling of these structures by caveolin-1 when cells are main-

tained in growth medium (A–C). In fixed cells it is apparent that LAMP-1 is localized on the surface of the LE/lysosomes and that caveolin-1 has a similar distribution and is localized at the LE/lysosomal outer membrane (arrows in Supplemental Figure S2, D and E). This provides further evidence that caveolin-1 is not in the lumen of the lysosome. Endogenous caveolin behaves similarly, and Supplemental Figure S2, G–I, shows the colocalization of endogenous caveolin detected with a polyclonal anti-caveolin antibody and LAMP-1.

Raising the intralysosomal pH traps caveolin at LE/lysosomes

How does starvation trigger the accumulation of caveolin on the lysosome? Because pH is a key mediator of lysosome function, we

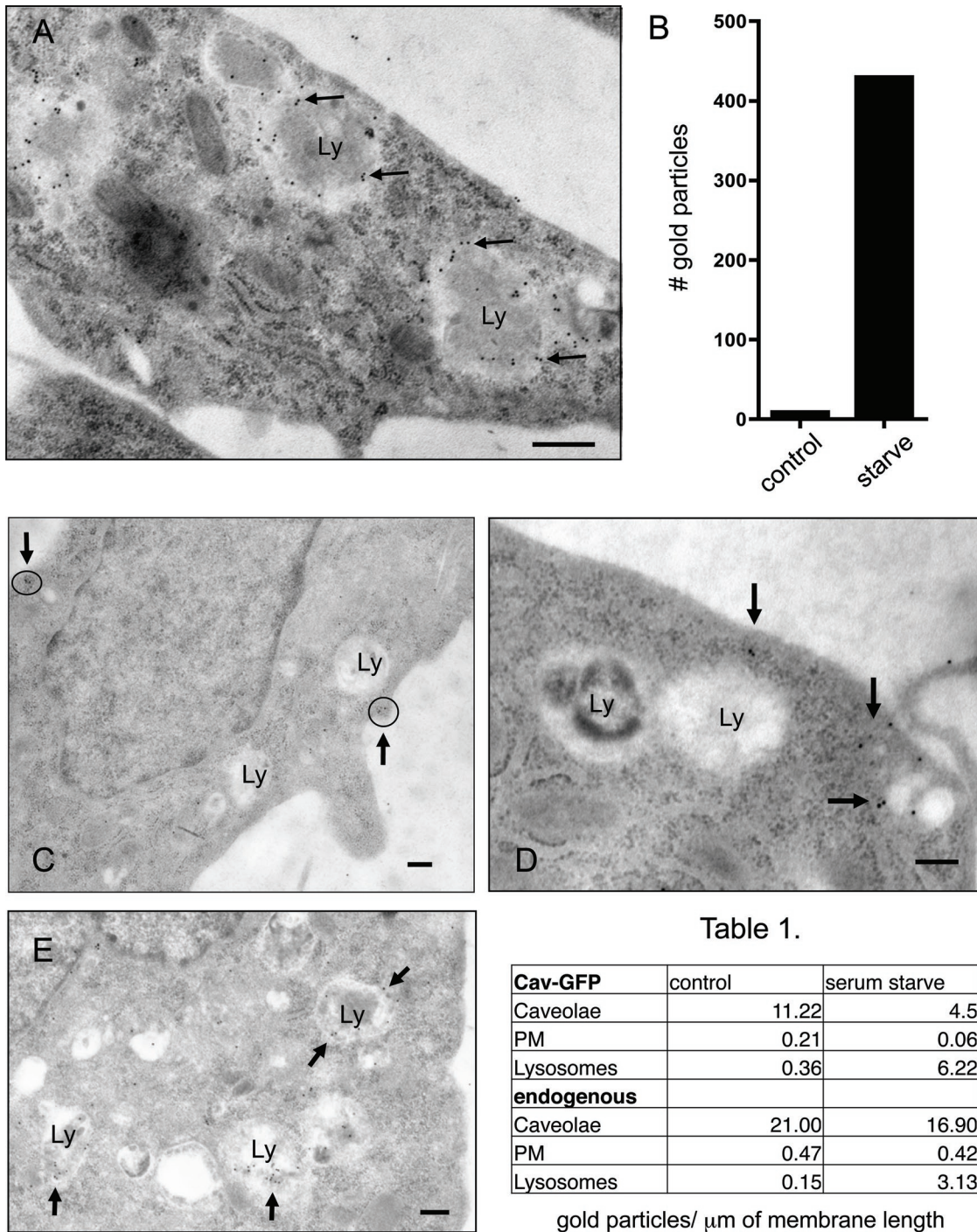


FIGURE 2: Electron microscopy confirmed that both endogenous and caveolin-1-GFP are recruited to LE/lysosomes upon serum starvation. Stably transfected CHO cells grown in growth medium or serum starved overnight were fixed as described in *Materials and Methods*. (A) Starved cells were labeled with an anti-GFP antibody. Caveolin labeling is localized primarily to the limiting membrane of the lysosome (Ly). The bar graph represents the number of gold particles that were associated with 50 lysosomes from either control or cells that were starved overnight. (C–E) Untransfected CHO K1 cells were maintained in growth medium (C, D) or starved overnight (E) before fixing and processing for immunogold labeling with a polyclonal anti-caveolin antibody. In growth medium caveolin is located at the plasma membrane in caveolae (C, circles with arrows; D, arrows) with no apparent labeling of lysosomes. (E) In serum-free medium endogenous caveolin also shows a dramatic redistribution to and colocalization with LE/lysosomes (arrows). Scale bar, 0.2 μm . Quantification of the gold label shows a decrease in caveolae at the PM and an increase of caveolin on the LE/lysosomal membrane in both the stable cell line expressing caveolin-1-GFP and untransfected CHO cells (Table 1; see Supplemental Table 1 for details).

tested whether serum starvation altered the intralysosomal pH, using ratiometric fluorescence microscopy. To measure the pH of individual lysosomes in serum-starved and control cells, we loaded lysosomes

with fluorescently labeled dextrans by endocytosis (Bayer et al., 1998). We used two different methods to determine the pH of the dextran containing organelles. In the first method we used both

fluorescein isothiocyanate–dextran (FITC-dex; pKa = 6.4) and Oregon green dextran (OG-dex; pKa = 5.0). When these probes are excited at 440 nm the fluorescence is pH independent, whereas the fluorescence of both probes at 488-nm excitation changes as a function of pH. Because the pKa values of the two fluorophores are different, combining the two dyes allows measurement of pH across the physiological range (Christensen *et al.*, 2002). The second method used a dextran that was coupled to both FITC and rhodamine (FITC/RH-dex). FITC fluorescence decreases at acidic pH, whereas rhodamine fluorescence is pH independent. Therefore the ratio of FITC/rhodamine fluorescence intensity is pH dependent (Majumdar *et al.*, 2007). The pH of the LE/lysosomal compartments was determined from the ratios measured by comparison with a standard curve (Supplemental Figure S3A), where lysosomal pH was fixed by the proton ionophores nigericin and valinomycin.

The fluorescence intensity ratios from ~3000–4000 LE/lysosomes were measured in each experiment in CHO cells loaded with fluorescent dextrans and maintained either in growth medium or serum-free medium. The mean pH of the LE/lysosomes of cells labeled with OG-dex/FITC-dex and maintained in growth medium from two separate experiments was 5.4 ± 0.2 . Starvation shifted the mean lysosomal pH upward by more than one unit, to 6.6 ± 0.3 . Similar results were obtained using cells labeled with FITC/RH-dex: the apparent lysosomal pH shifted from 4.8 ± 0.3 in cells maintained in growth medium to 5.9 ± 0.4 in serum-starved cells (Figure 3A).

Because serum starvation increased the pH of the lysosome, we tested whether other reagents that increase the pH of acidic organelles could cause the redistribution of caveolin-1 to LE/lysosomes. When CHO cells stably expressing caveolin-1-GFP were treated with the ionophore monensin (Marsh *et al.*, 1982; Wileman *et al.*, 1984), caveolin-1 rapidly translocated to a compartment resembling the one observed in serum-starved cells (Figure 3B). Within minutes, caveolin-1 began to accumulate on vesicles in the cytoplasm of the cell, and these compartments were strongly labeled by 10–20 min (Figure 3C). As in starved cells, only a subset of the caveolin-1-GFP is recruited to these vesicles, and caveolin-1-GFP also remains associated with the cell surface. To show that these structures were LE/lysosomes, we loaded lysosomes of CHO cells with Alexa 595–labeled dextran and then incubated with monensin (Figure 3D and E). Caveolin-1 colocalized with Alex 595–dextran, suggesting that caveolin-1 translocates to LE/lysosomes when the pH of the LE/lysosomal lumen is elevated.

To confirm this, we used bafilomycin A1, an inhibitor of the vacuolar proton pump, to raise the intralysosomal pH (Yoshimori *et al.*, 1991; Bayer *et al.*, 1998; Christensen *et al.*, 2002). When cells were treated with 100 nM bafilomycin, caveolin-1-GFP rapidly translocated to LE/lysosomes (Figure 3F). This translocation occurred with the same kinetics observed with monensin treatment (10–20 min). Similar results were observed with both CHO cells and the fibroblast cell line SV589. The identity of the compartments in SV589 cells as LE/lysosomes was confirmed by transfecting these cells with caveolin-1-GFP, incubating the cells in the presence of bafilomycin, and staining the cells with anti-LAMP-1 IgG (Figure 3, G–I). As with CHO cells, caveolin-1-GFP accumulated on vesicles that were LAMP-1 positive only when cells were serum starved. Fluorescence ratiometric measurements showed that bafilomycin treatment raised the pH of LE/lysosomes to 7.0, which is consistent with previous reports. These results indicate that dissipation of the lysosomal pH causes rapid redistribution of caveolin-1 to LE/lysosomes.

One trivial explanation for our results both in serum-starved and monensin- or bafilomycin-treated cells would be that the caveolin-1-GFP is already located in the LE/lysosomes but the GFP signal is

quenched by the low lysosomal pH (Patterson *et al.*, 1997). To show that this was not occurring, we took advantage of the fact that we could clamp the pH of cells, as we did to generate the pH curves used to measure lysosomal pH, and look at the effect of pH on caveolin-1-GFP in situ (see *Materials and Methods*). In control cells there was no sudden appearance of a GFP signal in LE/lysosomes at any pH between 4 and 7. Conversely, when serum-starved cells were clamped at low pH (5.5) or high pH (7.5) the total signal was reduced at pH 5.5 but was still clearly visible (Supplemental Figure S3B).

The association of caveolin with LE/lysosomes is reversible, and caveolin is not degraded

Further evidence that this is a bona fide pathway for caveolin trafficking is the observation that the association of caveolin with LE/lysosomes is rapidly reversible. Starved CHO cells stably expressing caveolin-1-GFP were imaged by time-lapse microscopy after the addition of growth medium. The caveolin-1-GFP associated with LE/lysosomes began to disappear within minutes and was essentially gone by 15 min (Figure 4A and Supplemental Video S4). The total fluorescence did not change, indicating that there was no significant photobleaching. To examine this rapid reversal further, we used a DeltaVision deconvolution microscope with point visiting capability to determine where caveolin-1 went after leaving LE/lysosomes. Stably transfected CHO cells were starved overnight, and at the start of the experiment 10 random fields were selected and a through-focus z-stack was taken of each area. The starvation medium was then replaced with fresh growth medium, the same 10 fields were revisited, and a second stack of images was taken. In all fields, caveolin-1-GFP was no longer associated with LE/lysosomal structures after 15 min in growth medium (Figure 4, compare B and C). We showed that at least some of the caveolin was translocated to the plasma membrane by quantifying the amount of caveolin along one edge of the cell (arrowheads). In the example shown, both the total intensity of GFP fluorescence and the density of GFP puncta were increased after 15 min in growth medium (Figure 4D, compare top and bottom graphs), whereas fluorescence on the lysosomes disappeared nearly completely. By quantifying all 10 fields we determined that the mean fluorescence intensity on the plasma membrane was increased by $43 \pm 4\%$ (SEM) after reversal (see *Materials and Methods*).

To quantify the change in the association of caveolin-1-GFP with lysosomes, we determined the Pearson coefficients for colocalization of GFP and LysoTracker in cells that were maintained in growth medium or serum starved overnight. Representative confocal images of cells labeled with both LysoTracker and caveolin-1-GFP at time zero and 15 min after replacing the starvation medium with growth medium were analyzed. The Pearson correlation coefficients determined for these images showed little or no colocalization between LysoTracker and caveolin-1-GFP in control cells ($r = 0.15$) and no colocalization in cells where the starvation medium was replaced with growth medium ($r = 0.64$). As expected, there was a highly significant positive correlation in the serum-starved cells ($r = 0.14$; Figure 4E).

To confirm that caveolin was not being degraded, we immunoblotted total cellular extracts from control cells, serum-starved cells, or cells that were serum starved and then reversed by being placed in growth medium for 15 min, and we found that the total amount of both endogenous caveolin and caveolin-1-GFP was unchanged (Figure 5A). The turnover of caveolin is known to be slow (days), and so to further establish that our treatments had no effect on the turnover of caveolin-1 we pulse labeled cells with

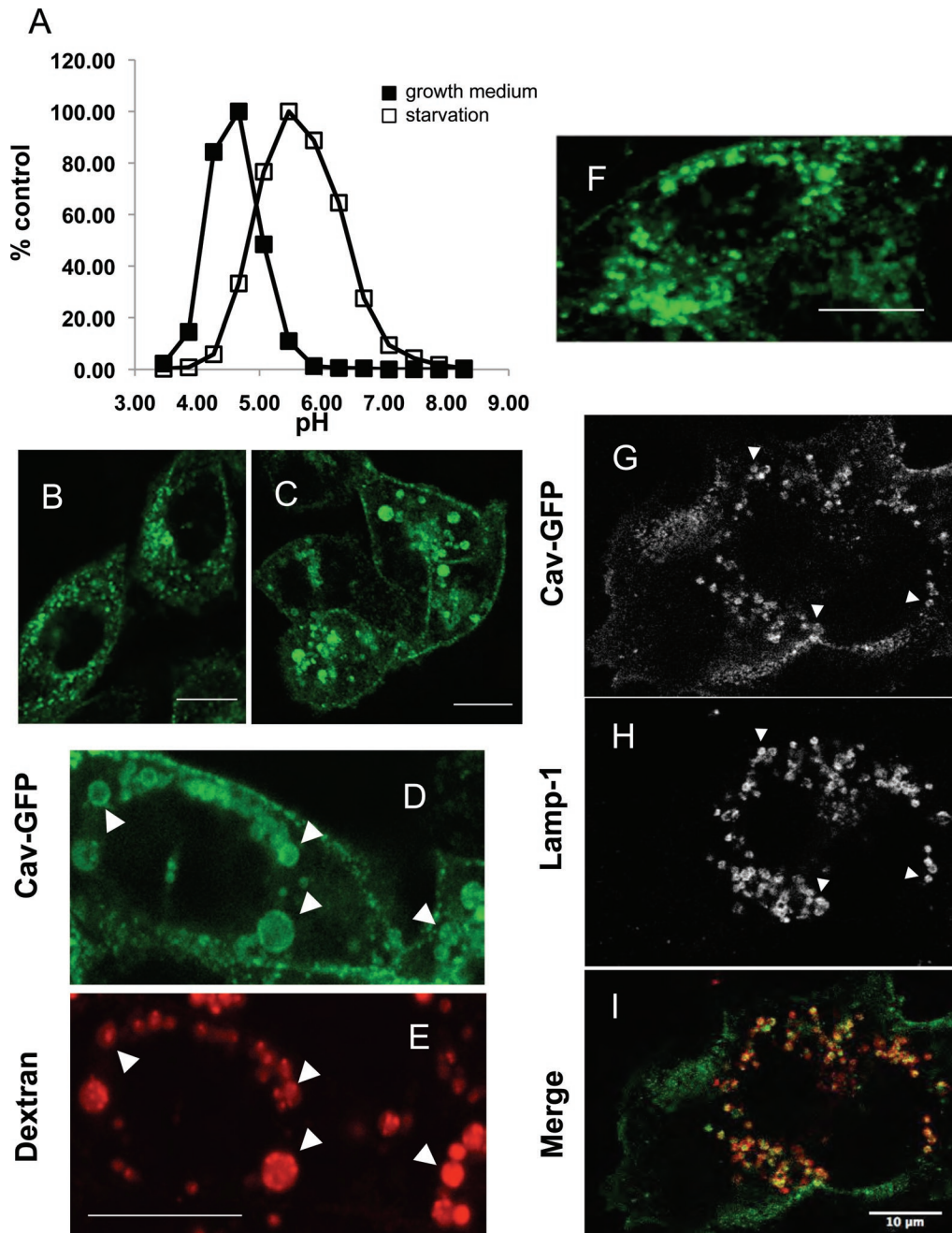


FIGURE 3: The intralysosomal pH is increased in starved cells, and drugs that increase the pH of lysosomes redistribute caveolin to LE/lysosomes. (A) CHO K1 cells were loaded with a 70,000-molecular weight dextran double labeled with FITC and rhodamine at 1 mg/ml in either growth or serum-free medium and chased for 2.5 h to accumulate the dextran in LE/lysosomes. LE/lysosomal pH was determined as described in *Materials and Methods*. The mean pH of LE/lysosomes in control cells was 4.8, whereas the mean pH of the LE/lysosomes in cells that were serum starved was shifted higher to 5.9. (B–E) CHO cells stably expressing caveolin-1-GFP were treated with the ionophore monensin (25 μ M) and imaged by time-lapse confocal microscopy. Within minutes caveolin began to accumulate on vesicular structures, and by 20 min this compartment was clearly labeled with caveolin-1-GFP. (B) A total of 94% of the cells showed this redistribution, and this experiment was performed at least eight times. (C) By 60–90 min of treatment with monensin the structures become large and distended, and caveolin-1-GFP remained associated with these large structures. (D, E) Cells were preloaded with 0.3 mg/ml of Alexa 595-dextran for 1 h and chased for 1 h before being treated with monensin for an additional hour. The extensive colabeling of the structures by both caveolin-1-GFP and the fluorescently tagged dextran demonstrates that these structures are LE/lysosomes (arrows). (F) CHO cells were treated with 100 nM bafilomycin and imaged by time-lapse microscopy. Again caveolin-1-GFP redistributes to LE/lysosomal compartments within 10–20 min in the presence of the drug. (G–I) SV589 human fibroblasts transfected with caveolin-1-GFP for 24 h were treated with 100 nM bafilomycin for 30 min, fixed, and labeled with an anti LAMP-1 antibody. The arrows indicate caveolin-1-GFP on LAMP-1-positive structures, establishing that these structures are LE/lysosomes. At least 95% of the cells showed this redistribution, and the experiment was performed three times with CHO cells and twice with SV589 cells. Scale bars, 10 μ m.

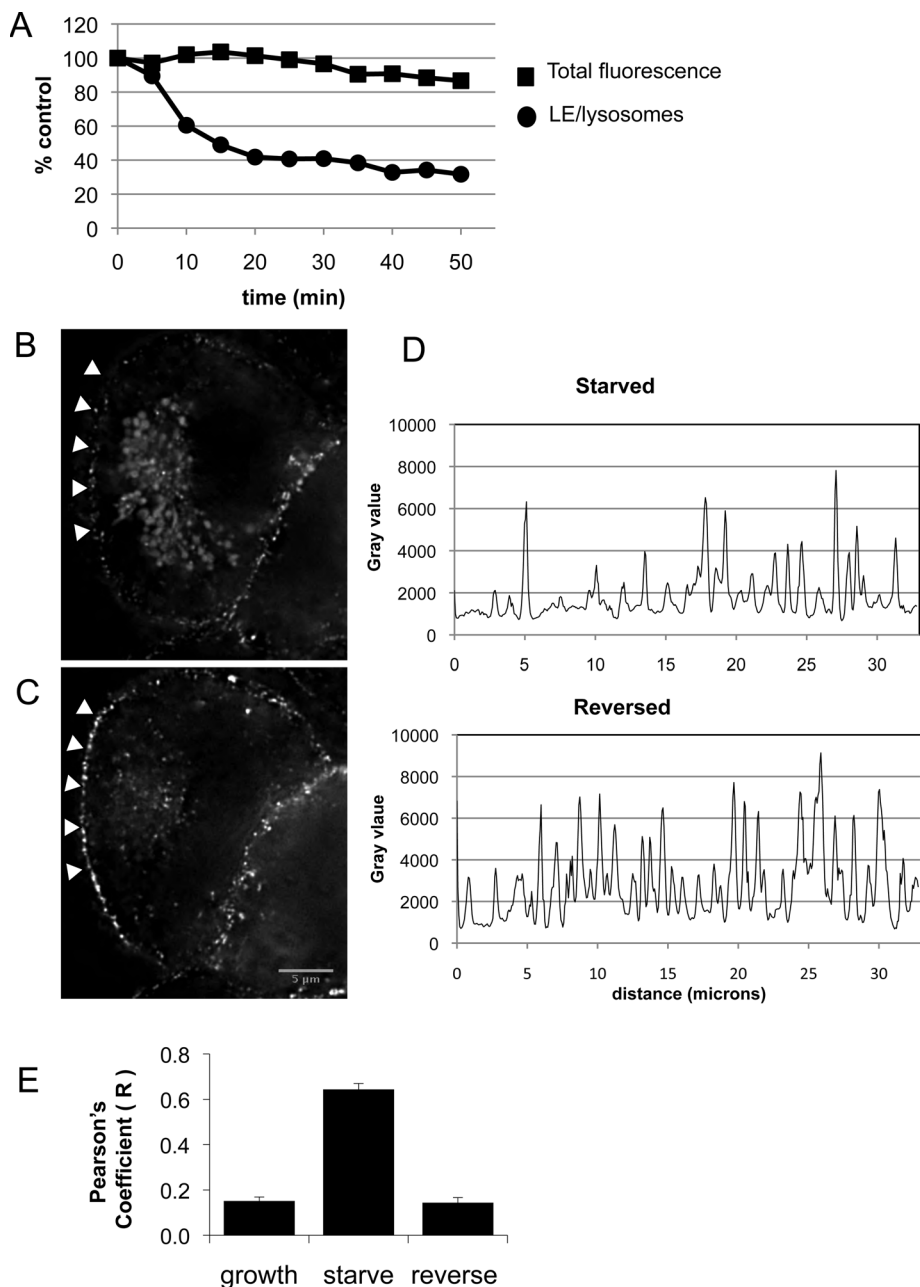


FIGURE 4: Caveolin association with LE/lysosomes is rapidly reversed upon addition of growth medium, with a concomitant increase in plasma membrane labeling. Stably transfected CHO cells were serum starved overnight. (A) At time zero the starvation medium was replaced with warm growth medium, and the cells were imaged every 5 min by time-lapse confocal microscopy. The total GFP fluorescence was measured over the areas that contained LE/lysosomes and from the entire area at each time point and plotted on the graph. Caveolin-1-GFP dissociated from the LE/lysosomes within minutes and reverted to its normal distribution by 15–20 min (see also Supplemental Video S4). (B, C) At the start of the experiment a stack was taken from 10 areas using a DeltaVision deconvolution microscope. The starvation medium was replaced with fresh growth medium, and after 15 min the same 10 fields were revisited. A representative image of a cell before and after reversal shows that caveolin-1-GFP is no longer associated with LE/lysosomes. At least some of the caveolin relocated to the plasma membrane as shown in the graphs. (D) A plot profile was generated from the edge of the cell (arrowheads) and demonstrated there was a dramatic increase in the number of peaks after reversal measured in arbitrary fluorescence units (gray value). (E) Stably transfected cells were labeled with 50 nM LysoTracker for 30 min, and colocalization between caveolin-1-GFP and LE/lysosomes was determined as described in *Materials and Methods*. The bar graph shows the Pearson's coefficient calculated for each condition and indicates that caveolin is only colocalized with LE/lysosomes in starved cells and is no longer associated after a short incubation with fresh growth medium. We analyzed 13, 15, and 21 cells, respectively, for control, starved, and reversed cells.

^{35}S -cysteine/methionine and chased in the presence of cold amino acids for up to 28 h. Figure 5B shows that starvation has no effect on the turnover of either endogenous caveolin-1 or caveolin-1-GFP. We conclude that accumulation of caveolin-1-GFP on LE/lysosomes is reversible and that caveolin-1 is not being degraded as a consequence of its localization to LE/lysosomes.

These results contrast with PTRF/cavin1-controlled degradation of caveolin-1. Hill *et al.*, (2008) showed that caveolin is degraded by lysosomes when PTRF/cavin1 was knocked down, which is consistent with the findings in PTRF-negative mice, which also have little or no caveolin (Liu and Pilch, 2008). The authors suggested that PTRF knockout results in the slow degradation of caveolin because PTRF is required to stabilize caveolin on the cell surface. Without it, caveolin-1 enters cells via the bulk endocytic pathway and is translocated to the lumen of the lysosomes just like other bulk markers such as dextran and receptors destined for degradation. To determine whether PTRF plays a role in the translocation of caveolin-1 to LE/lysosomes, we immunoblotted extracts from cells that were maintained in growth medium or starved overnight for both PTRF and caveolin and found no decrease in the levels of either protein (Supplemental Figure S4A). More important, when we coexpressed tagged versions of caveolin-1 and PTRF, we found that the two proteins colocalized at the plasma membrane in cells maintained in growth medium; however, when cells were starved, caveolin-1-GFP translocated to the LE/lysosomes, but PTRF remained at the cell surface in puncta that also contained caveolin-1 (Supplemental Figure S4B). These data demonstrate that the starvation-induced translocation of caveolin to LE/lysosomes is distinct from the PTRF-dependent degradation pathway.

Role of cholesterol in caveolin-1-GFP recruitment to LE/lysosome membranes

Both serum starvation and elevated lysosomal pH reduce the availability of cholesterol in LE/lysosomes for transport to other cellular compartments (Brown and Goldstein, 1986; Furuchi *et al.*, 1993). A third condition that interferes with the transport of cholesterol out of LE/lysosomes is exposure of cells to either progesterone (McGookey and Anderson, 1983; Butler *et al.*, 1992) or U18666A (Cenedella, 2009). U18666A and progesterone both block the exit of cholesterol from lysosomes, although

their mechanism of action is not known. CHO cells stably expressing caveolin-1-GFP were pretreated with either progesterone (Figure 6, A–C) or U18666A (Figure 6, D–F) for 16 h before they were loaded with LysoTracker (Figure 6, B and E) and examined by live-cell microscopy. Both drugs caused a dramatic accumulation of caveolin-1-GFP around LysoTracker-positive compartments (merge in Figure 6, C and F). As expected, these compartments are also positive for filipin, a fluorescent polyene macrolide used to detect free cholesterol in cells (Figure 6, G–I). As with serum-starved cells, the immunofluorescence images show that caveolin is on the limiting membrane of the LE/lysosomes and not in the lumen (Figure 6, A, D, and H). More important, we showed that treatment with U18666A had no effect on the turnover of either endogenous caveolin-1 or caveolin-1-GFP (Figure 5B), proving that caveolin was not being shunted into the degradation pathway.

We obtained additional evidence that cholesterol is important in the redistribution of caveolin-1-GFP to LE/lysosomes by treating cells with methyl- β -cyclodextrin (M β CD). Cyclodextrins have been extensively used to deplete cells of cholesterol (Rodal *et al.*, 1999; Roy *et al.*, 1999; Parpal *et al.*, 2001; Le *et al.*, 2002). When our stable cell line was treated with low concentrations (0.1–0.3%) of M β CD overnight, caveolin-1-GFP again accumulated at the limiting membrane of LE/lysosomes (Figure 7, A–C). In general, higher concentrations of cyclodextrin are used to rapidly deplete cholesterol, but we found that at those concentrations (1% M β CD) the caveolin-1-GFP signal becomes diffusely distributed in the plasma membrane within 20–30 min, and caveolin-1-GFP is not associated with LE/lysosomes (Figure 7, D–F). In addition, cells do not survive overnight treatment with these higher concentrations of M β CD, whereas cells are relatively unaffected by the lower concentrations.

Although the caveolin-1-GFP positive rim around each vesicle was similar to what we observed with serum starvation and elevated pH, there was one notable difference. In contrast to starved cells, cavicles appeared to be docked on LysoTracker- or dextran-positive LE/lysosomes in both progesterone- and U18666A-treated cells and in cells treated with M β CD (Figures 6, A and D, and 7A). This is much more apparent in the videos (see Supplemental Videos S5–S7) and suggests that cavicles may be involved in delivering and retrieving caveolin-1-GFP from LE/lysosomes under these conditions. In starved cells caveolin appeared more uniformly distributed around the limiting membrane of the LE/lysosome, and there was little evidence of cavicles docked at the lysosome periphery (compare Supplemental Video S1 with Supplemental Videos S5–S7). Taken together, these experiments suggest that altering the cholesterol availability at the LE/lysosome causes caveolin-1 to associate with or be trapped on the cytoplasmic surface of this organelle.

Finally, we determined whether free cholesterol accumulates in LE/lysosomes in starved cells. In cells maintained in growth medium, filipin stains the plasma membrane, but there is little staining of any internal cellular organelles. A similar staining pattern was seen in starved cells, indicating that there is no dramatic change in the localization of free cholesterol in the lysosomes of starved cells (Supplemental Figure S5, A and C). As expected, exposure to either progesterone or U18666A showed marked filipin staining of the LE/lysosomal compartment (Supplemental Figure S5, B and D). It is not surprising that free cholesterol does not accumulate in LE/lysosomes in starved cells since the lysosomal acid lipase that cleaves cholesterol ester to free cholesterol shows maximal hydrolysis at pH 4.4, and hydrolysis is negligible when the pH is raised to 6.0 (Koster *et al.*, 1980). We also determined that neither progesterone nor U18666A shifted the pH of the LE/lysosomes significantly from that of control cells (data not shown).

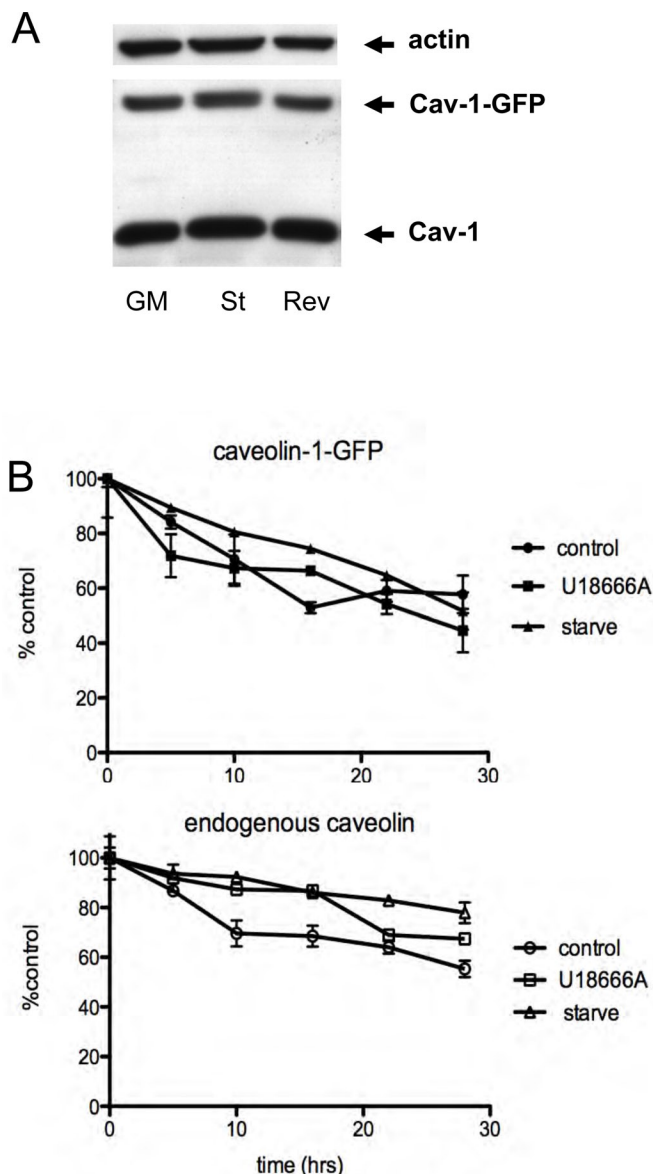


FIGURE 5: The degradation rate of caveolin is not altered by either starvation or treatment with U18666A. (A) Laemmli sample buffer was added directly to CHO cells that were maintained in growth medium or starved overnight \pm growth medium for 15 min (reverse) to make total cell lysates, and the extracts were analyzed by Western blotting using anti-caveolin antibodies. Neither caveolin-1-GFP nor endogenous caveolin was degraded under these conditions. Actin served as a load control. (B) Cells stably expressing caveolin-1-GFP were labeled with ^{35}S -Cys/Met in order to look at the turnover rate of both endogenous caveolin and the expressed caveolin-1-GFP as described in *Materials and Methods*. After the 2-h labeling period cells were chased in growth medium for 30 min and then switched to serum-free medium or kept in growth medium with or without U18666A (2.5 $\mu\text{g}/\text{ml}$). The rate of turnover for caveolin-1-GFP was faster than that for the endogenous protein, but neither U18666A nor serum starvation increased the degradation rate compared with control.

Genistein blocks arrival of caveolin-1 at LE/lysosomes but not reversal

When caveolin-1-GFP is stably expressed in cells we routinely find internal structures that contain caveolin and appear to have cavicles attached at their rims. These structures do not colocalize with any

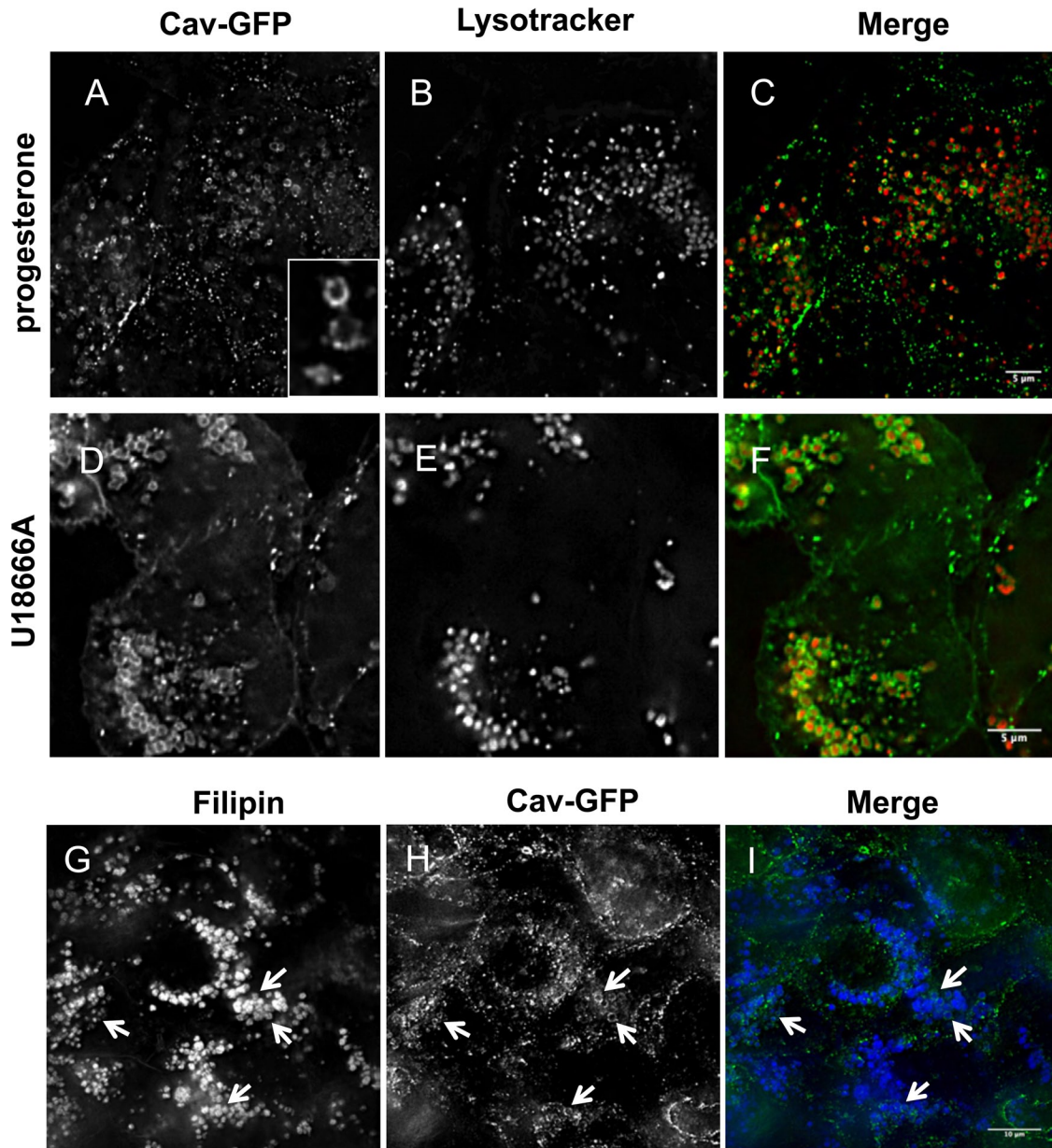


FIGURE 6: Caveolin redistributes to LE/lysosomes when cholesterol egress is blocked by progesterone or the drug U18666A. Stably transfected CHO cells were treated with either 10 $\mu\text{g/ml}$ progesterone (A–C) or 2.5 $\mu\text{g/ml}$ U18666A (D–F) overnight before labeling with 50 nM LysoTracker for 30 min and visualizing by live-cell microscopy. Caveolin-1–GFP redistributed to LE/lysosomes after each of these treatments. Ninety-six percent of the cells showed this redistribution, and the experiments were repeated >10 times. The structure of the caveolin appears to be somewhat different from that observed after starvation since rings are clearly visible and cavicles can be seen associated with these structures (see inset and Supplemental Videos S5 and S6). (G–I) Both progesterone and U18666A cause the accumulation of free cholesterol in LE/lysosomes. Cells treated with progesterone were fixed and stained with 50 $\mu\text{g/ml}$ filipin before mounting and imaging. Filipin-stained LE/lysosomes that have accumulated cholesterol, and caveolin-1–GFP is clearly associated with the periphery of these filipin-stained structures (arrows).

markers for the Golgi or the endoplasmic reticulum (ER). A number of articles (Pietiainen *et al.*, 2004; Damm *et al.*, 2005; Karjalainen *et al.*, 2008) described these structures and called them caveosomes, although their existence has recently been called into question (Hayer *et al.*, 2010). As has been reported, these are neutral compartments and do not label with either LysoTracker or dextran, indicating that they are not LE/lysosomes. Figure 8, A–C, shows still images taken from Supplemental Video S3 to demonstrate that these structures are not labeled with LysoTracker (arrows). Cavicle

delivery to and budding from these caveosomes is readily detected, and we had no difficulty imaging cavicles budding from these structures in cells (arrow in Figure 8D; Supplemental Video S8).

Therefore, if cavicles were involved in the disappearance of caveolin-1–GFP from the LE/lysosome during reversal after serum starvation, we would expect to detect cavicle budding from LE/lysosomes. This was not the case (Supplemental Video S4). We used fluorescence recovery after photobleaching (FRAP; Figure 8E and Supplemental Video S9) to see whether we could detect the delivery of

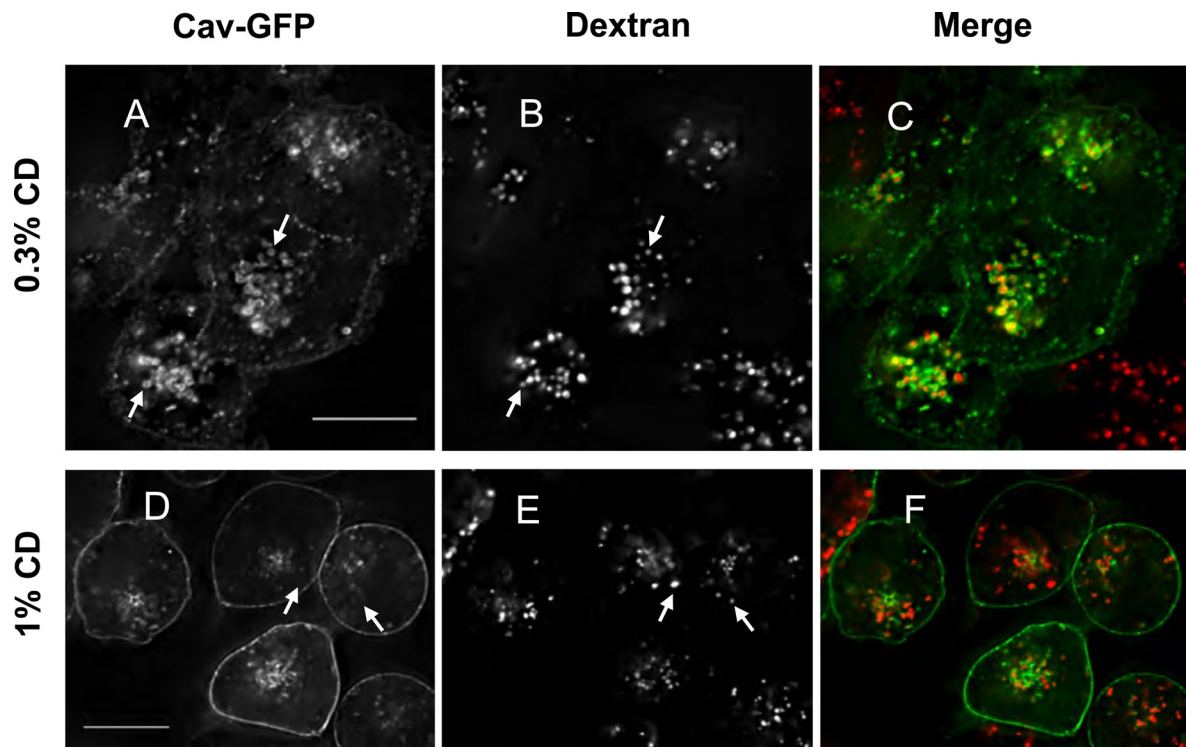


FIGURE 7: Caveolin redistributes to LE/lysosomes when cellular cholesterol is perturbed by low concentrations of M β CD. CHO cells stably transfected with caveolin-1-GFP were plated onto glass-bottomed dishes in growth medium 2 d before the cells experiment. One day before, cells were labeled with 0.15 mg/ml dextran in growth medium \pm 0.3% M β CD for 16 h and chased for 4 h in fresh growth medium \pm 0.3% M β CD (A–C). Cells that had been loaded with dextran overnight were treated with 1% M β CD for 30 min before imaging (D–F). At least 94% of the cells showed this pattern of redistribution, and the experiment with low concentrations of cyclodextrin was repeated 4 times and the ones with high concentrations 12 times. Scale bars, 10 μ m.

caveolin-1-GFP to LE/lysosomes in serum-starved cells. CHO cells were incubated in the absence of serum in order to accumulate caveolin-1-GFP on LE/lysosomes. An area of the cell where caveolin-1-GFP-positive LE/lysosomes were concentrated was bleached (Figure 8E, 0 min) by a short exposure to high-intensity laser light and monitored for recovery of the fluorescence intensity over time. No recovery occurred by 7.5 min (Figure 8E, 7.5 min). In fact, even with longer incubation times of up to 1 h, we did not see any recovery. This indicates that in serum-starved cells caveolin is not cycling on and off of the LE/lysosomal membrane. This contrasts with our previously published studies, in which we observed recovery within 5 min after bleaching areas of the cell that accumulate caveosomes (Mundy *et al.*, 2002). These experiments suggest that caveolin-1-GFP transport away from LE/lysosome may not involve cavicles and that caveolin is trapped on the LE/lysosome when cells are starved of serum.

Genistein has been used to block or at least slow the budding of caveolae/cavicles from the plasma membrane (Sharma *et al.*, 2004; Damm *et al.*, 2005; Cheng *et al.*, 2006b). We examined the effect of pretreatment with this inhibitor for 30–60 min before reversing by the addition of growth medium and found that genistein did not block reversal (data not shown). To determine whether genistein blocks trafficking of caveolin to LE/lysosomes we preincubated cells for 30 min with 50 μ M genistein and then added monensin for 1 h. Monensin induced the redistribution of caveolin to the LE/lysosome, and genistein blocked this redistribution (Figure 9, A–C compared with D–F). Genistein also blocked the redistribution of caveolin to LE/lysosomes induced by U18666A (Figure 9, G and H). These observations indicate that

caveolin traffics to LE/lysosomes by a tyrosine kinase-dependant process but that caveolin returns from LE/lysosomes by a different mechanism.

DISCUSSION

Caveolin-1 is a coat protein of caveolae. Whereas caveolin-1 plays a role in caveolae endocytosis (Le *et al.*, 2002; Singh *et al.*, 2003), several studies suggest that caveolin-1 also plays a key role in intracellular cholesterol trafficking and homeostasis. First, a number of studies have shown that caveolin is involved in the efflux of free cholesterol from cells (Fielding and Fielding, 1995; Fielding *et al.*, 2004; Smart *et al.*, 1996; Fu *et al.*, 2004). Second, a truncation mutation of caveolin acts as a dominant negative to induce a cholesterol trafficking defect that results in the depletion of cholesterol from the plasma membrane (Roy *et al.*, 1999; Pol *et al.*, 2001). Third, caveolin is required to maintain normal free cholesterol levels in lipid droplets of adipocytes, and this requires endocytosis of caveolae (Le Lay *et al.*, 2006). Fourth, in the absence of caveolin, free cholesterol appears to accumulate in mitochondrial membranes, which results in mitochondrial dysfunction and defects in metabolism (Bosch *et al.*, 2011). Our discovery that caveolin-1 can reversibly collect on the cytoplasmic surface of LE/lysosomes in response to perturbations that impair cholesterol efflux from LE/lysosomes provides the first evidence that caveolin may participate in cholesterol traffic from lysosomes.

We speculate that caveolin-1 normally traffics to and from LE/lysosomes but is not detected owing to the short time it spends there. This fits well with the evidence that caveolin-1 is involved in intracellular cholesterol transport, since LE/lysosomes are a source

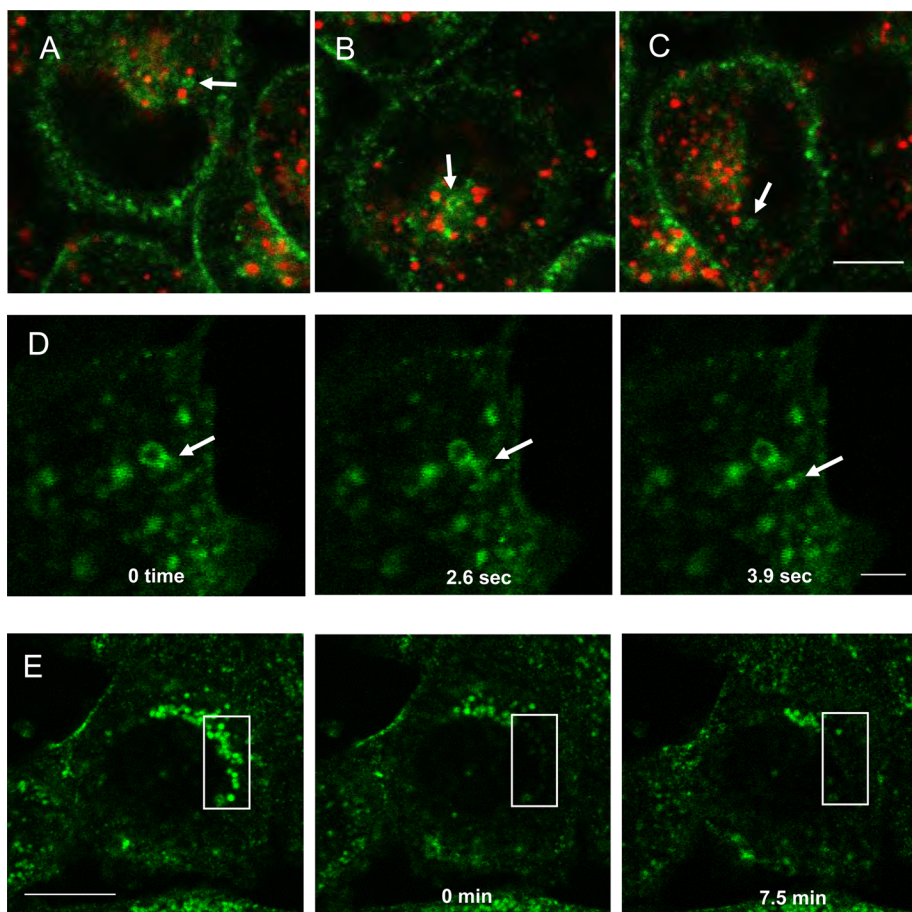


FIGURE 8: Visualization of caveosomes, cavicles, and caveolin-1-GFP trafficking in live cells. The trafficking of caveolin was visualized in CHO cells stably expressing caveolin-1-GFP and labeled with 50 nM LysoTracker for 30 min using time-lapse microscopy. These are selected frames from Supplemental Video S3 showing that caveosomes are not labeled by LysoTracker (A–C, arrows). (D) Frames from Supplemental Video S8 showing a cavicle (arrow) leaving a putative caveosome. Although cavicle trafficking to and from caveosomes was readily observed, we could not detect cavicles leaving the LE/lysosomes when the accumulation of caveolin on LE/lysosomes was reversed by the addition of growth medium. (E) Starved cells were analyzed by FRAP to determine whether the caveolin was cycling on and off of LE/lysosomes. After bleaching a small area of the cell (box) there was no recovery of the fluorescence up to 7.5 min after the bleach (Supplemental Video S9). This experiment was repeated twice. Scale bar, A–C, 5 μ m; D, 2 μ m; E, 10 μ m.

of lipoprotein-derived cholesterol (Brown and Goldstein, 1986). The conditions that cause caveolin-1 accumulation are ones that interfere with the availability of LE/lysosome cholesterol to interact with caveolin-1. Serum starvation depletes the LE/lysosome of a source of cholesterol and increases the pH of the lysosomes. Elevated pH disrupts the function of NPC2 (Cheruku *et al.*, 2006; Babalola *et al.*, 2007), which is an intermediate in the transfer of lysosomal cholesterol out of the LE/lysosome (Liscum and Sturley, 2004; Infante *et al.*, 2008). Progesterone and U18666A prevent exit of cholesterol from lysosomes by an unknown mechanism, and cholesterol is most likely inaccessible to caveolin-1 under these conditions as well. There has been frequent speculation that progesterone and U18666A mimic the phenotype of Niemann–Pick type C disease, and there is evidence that the action of U18666A is dependent on NPC1 and NPC2. However, the ability of U18666A to cause cholesterol accumulation in LE/lysosome is not stereospecific, suggesting that its mechanism of action involves a general change in the physical properties of the membrane lipid bilayer rather than binding to a specific

protein (Cenedella, 2009). Thus, caveolin-1 may accumulate on LE/lysosomes under these conditions because cholesterol is not accessible or cannot be extracted owing to the altered physical properties of the lipid bilayer surrounding the LE/lysosome. Cyclodextrin at high concentrations rapidly removes cholesterol from the plasma membrane and does not result in the accumulation of caveolin on LE/lysosomes presumably because it stops caveolin trafficking completely. Interestingly, used at lower concentrations that have been shown to mobilize cholesterol from the lysosomes of NPC1- and NPC2-defective cells (Abi-Mosleh *et al.*, 2009; Rosenbaum *et al.*, 2010), caveolin-1 accumulated at the limiting membrane of LE/lysosomes. One possibility is that cholesterol homeostasis is perturbed, and this slows the trafficking of caveolin through the intramembrane system and it accumulates at one of its way stations. It is not known how cyclodextrins mobilize cholesterol from LE/lysosomes, but perhaps caveolin is involved.

Live-cell imaging suggests that caveolin-1 is transported to cholesterol-starved LE/lysosomes by both vesicular and non-vesicular mechanisms. Vesicular transport may be mediated by cavicles like those we observe budding from caveosomes (Figure 8A; Supplemental Video S8). Normally these would only transiently interact with LE/lysosomes, but they are trapped there when cholesterol egress is blocked, perhaps by the lack of available cargo. By analogy with LE-to-lysosome fusion (Bright *et al.*, 2005) and cavicle trafficking to early endosomes (Pelkmans *et al.*, 2004), we propose the interaction involves a kiss-and-run mechanism. We do see transient interactions of lysosomes with cavicles and are developing assays to investigate those interactions. The nonvesicular pathway may

involve interorganelle membrane contact sites between LE/lysosomes and other caveolin-rich sites such as the ER, caveosomes, or the plasma membrane. Transient contacts have been implicated in the transfer of phosphatidylserine from the ER to mitochondria (Voelker, 2003), mediated in part by a dynamin-related protein called mitofusion 2 (de Brito and Scorrano, 2008). Intracellular membrane contacts between ER and plasma membrane have also been described (Pichler *et al.*, 2001), which suggests that this is a common mechanism by which intracellular membrane compartments communicate. The transfer mechanism used by caveolin would be expected to differ from that proposed for these pathways, but caveolin may be uniquely suited to transfer between closely apposed membranes via transient tubules. This is because caveolin inserts exclusively into one leaflet of the lipid bilayer, as evidenced by the fact that caveolin can move in and out of lipid droplets that are attached to the ER, and droplets are surrounded only by a lipid monolayer (unpublished observations; Martin and Parton, 2005). Support for such a mechanism also comes from the

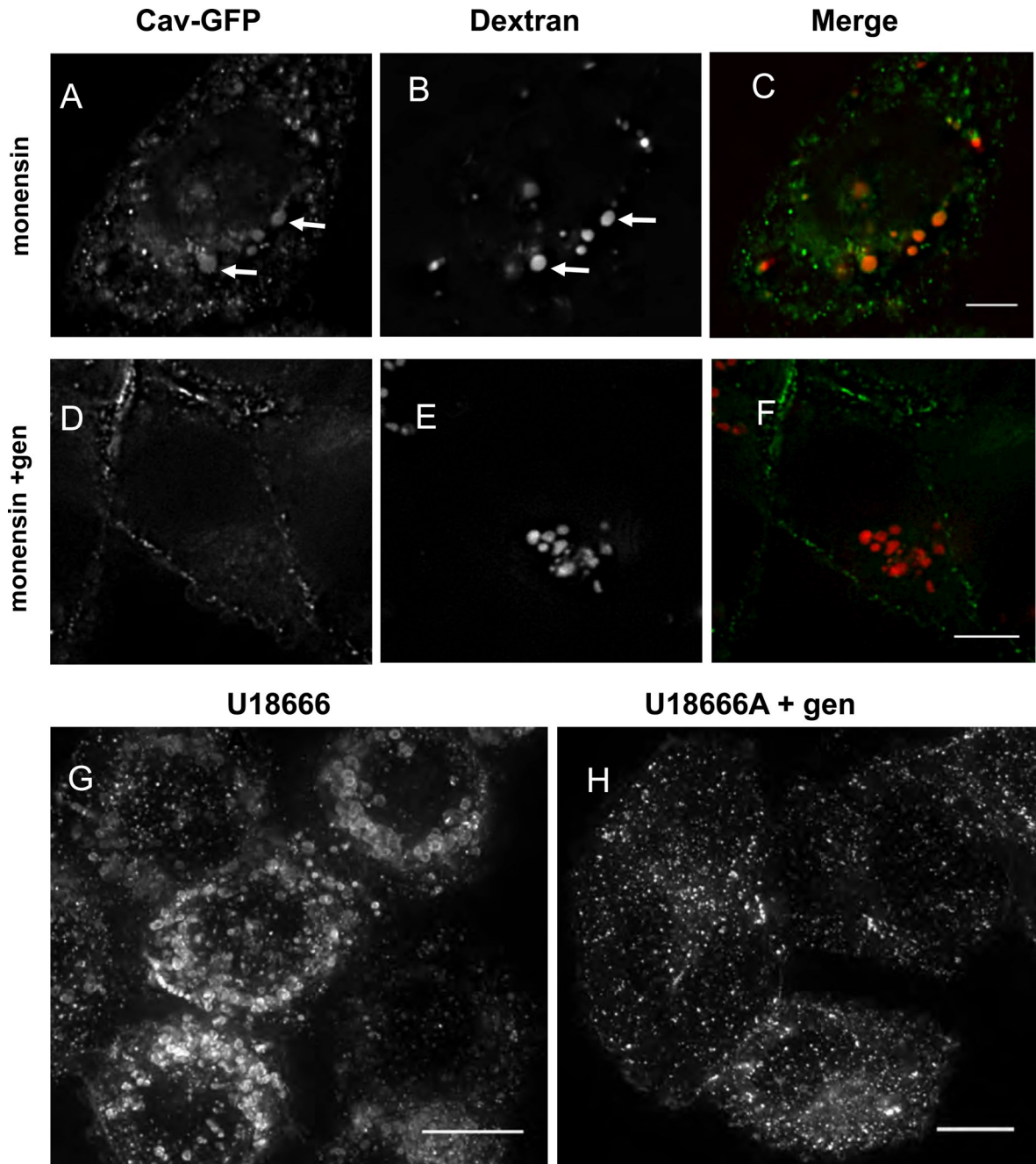


FIGURE 9: Genistein blocks the redistribution of caveolin to LE/lysosomes. CHO cells stably expressing caveolin-1-GFP were pretreated with 50 μM genistein for 30 min (D–F) or not (A–C) and then treated for an additional 1 h with 25 μM monensin to determine whether genistein could block the redistribution of caveolin to LE/lysosomes (images are single confocal slices). (G, H) Cells were either treated with 50 μM of genistein for 30 min or not, as indicated, before adding 2.5 $\mu\text{g/ml}$ U18666A overnight and were visualized by live-cell confocal microscopy. Images are maximum-intensity projections of the cells and show that genistein blocked the redistribution of caveolin to LE/lysosomes. We found no cells that showed redistribution in the presence of genistein. This experiment was repeated three times. Scale bars, 10 μm .

apparent ability of caveolin to tubulate membranes (Mundy *et al.*, 2002; Voeltz and Prinz, 2007; Verma *et al.*, 2010).

Although cell surface caveolae have been described for many years, the full extent of the caveolin membrane system was only recently discovered (Figure 10). It consists of flask-shaped caveolae, tubular caveolae, cavicles (caveolin-coated vesicles that shuttle between compartments), and the caveosome, a novel organelle. The existence of the caveosome has recently been called into

question by a study in which caveolins were transiently overexpressed and the exogenous caveolins were found to be degraded in lysosomes (Hayer *et al.*, 2010). The authors saw similar structures to those we describe here and suggested that these were the caveosomes they originally described in several papers (Pelkmans *et al.*, 2001, 2002, 2004; Damm *et al.*, 2005; Tagawa *et al.*, 2005). Hayer *et al.* (2010) show nicely that the normal degradation pathway for caveolin is via the LE/lysosome and requires ubiquitination,

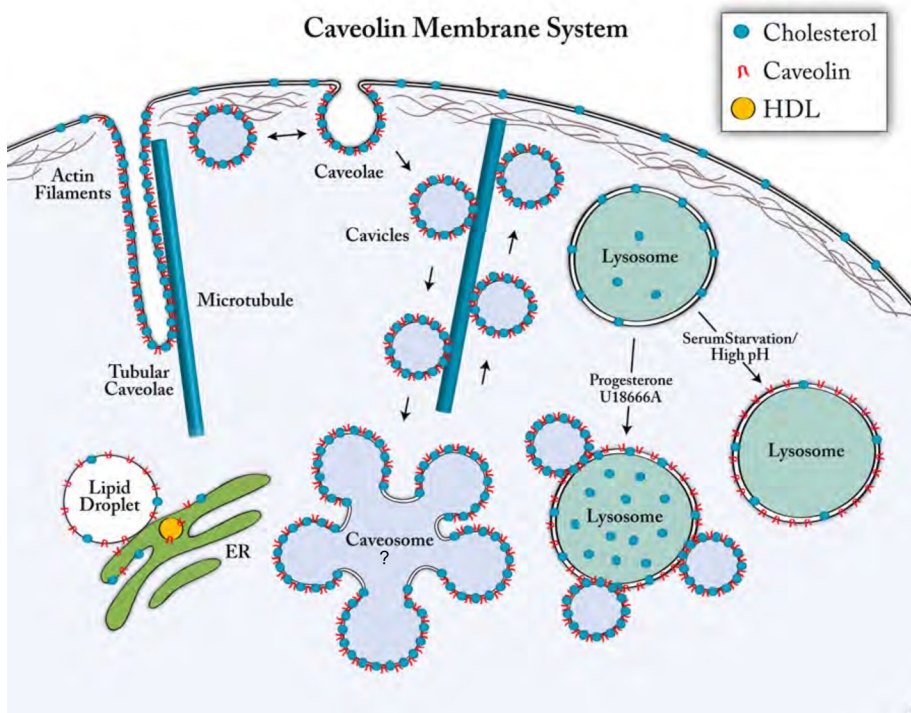


FIGURE 10: The caveolin membrane system. At steady state caveolin is located at the plasma membrane in caveolae, in a recently identified intracellular compartment called the caveosome, and on caveolin-coated vesicles (cavicles) that traffic between compartments. Under certain physiological conditions and in specialized cells caveolin can also be found on lipid droplets, on high-density lipoprotein particles that are secreted, and, as we show here, on LE/lysosomes. Newly synthesized caveolin is inserted into the ER, and caveolin then traffics using the conventional secretory pathway through the Golgi to the plasma membrane. At the ER and on lipid droplets caveolin is in the form of monomers or small oligomers, whereas at the plasma membrane and on caveosomes it forms a multimeric coat. The equilibrium between monomers and multimers is most likely controlled by the cholesterol levels in the various membranes. Caveolae are endocytosed from the plasma membrane, and caveosomes may act as a central clearinghouse for the trafficking between compartments, but we are only just beginning to understand this system. The caveolin membrane system communicates with the endosomal membrane system at two points. The first is a pathway from the plasma membrane to the early endosomes, where endocytosed cavicles briefly encounter (kiss and run) early endosomes and seem to exchange some cargos. The second is the one we describe here to the LE/lysosomes, which may also occur via a kiss-and-run mechanism when cells are maintained in growth medium, but when cells are starved or the lysosomal pH is dissipated the interaction appears to result in complete fusion and dissociation of the caveolin into monomers. Blocking egress of cholesterol by drugs, on the other hand, appears to trap intact cavicles on LE/lysosomes.

and degradation is increased by transiently overexpressing caveolins or by knocking down cavin1/PTRF. That is not, however, the explanation for why caveolin associates with LE/lysosomes under our conditions, where cholesterol homeostasis is perturbed. Indeed, we determined by metabolic labeling that neither endogenous caveolin nor the stably expressed caveolin-1-GFP is degraded at any greater rate in control, starved, or U18666A-treated cells. We also showed that the association of caveolin with LE/lysosomes is reversible and redistribution occurs within minutes when the pH of the lysosomes is increased by ionophores or proton pump inhibitors, before there could be any accumulation due to a blockage of degradation. In our hands caveosomes seem to be relatively few in number but are clearly not labeled by either LysoTracker or dextrans as was originally reported. In addition, they coexist with caveolin associated with LE/lysosomes, which are much more numerous, so it remains to be determined whether caveosomes are an artifact or a real entity.

transport with coat assembly and disassembly. Their model proposes a cycle of phosphorylation/dephosphorylation on Ser-80 in the caveolin molecule that would regulate coat assembly, but the model remains to be tested. The diffuse versus punctate pattern we see on LE/lysosomes might reflect whether caveolin is binding or releasing cholesterol.

We cannot be certain the conditions that cause caveolin-1 to accumulate on LE/lysosome membranes have anything to do with intracellular cholesterol transport. However, this new pathway for caveolin-1 trafficking fits well with the numerous data showing that caveolin-1 is involved in delivering cholesterol to various membrane compartments. Obviously caveolin-1 is not the only molecule involved in distributing cholesterol, because cells lacking this protein are viable. Of interest, caveolin-1-null mice have higher cholesterol esterification rates and lower cholesterol synthesis rates than wild-type mice, indicating that they have an imbalance in cholesterol homeostasis (Frank et al., 2006). Correct intracellular transport and

At the plasma membrane caveolae are generally distinct morphological entities, and this seems to be the case when caveolae/cavicles dock with some internal membranes as well. All indications are that cholesterol controls the structure of caveolae and that this might regulate the cargo exchange process. Depleting cholesterol causes caveolae to lose their integrity, and under those conditions caveolin is free to diffuse away from its normally stable association with a single caveolae (Tagawa et al., 2005). Our observations with caveolin-1-GFP are when cells are depleted of cholesterol using high concentrations of cyclodextrin; caveolin is no longer clustered in puncta at the cell surface but is evenly dispersed throughout the plasma membrane. It is of interest therefore that when caveolin translocates to the LE/lysosomes under high-pH conditions it has a similarly diffuse appearance and does not remain a discrete entity as it does when it fuses with the caveosome. The most likely explanation for this is that the cholesterol content of these membranes is low and caveolin is no longer able to either form or maintain the oligomers/multimers required to maintain the coat structure. Caveolin has a similar diffuse distribution when it is associated with lipid droplets. Our data are consistent with the idea that caveolin on the LE/endosomes in starved cells is in a monomeric/disassembled state. In contrast, when caveolin accumulates on LE/lysosomes in progesterone- or U18666A-treated cells the integrity of the cavicle is at least partially maintained, which might indicate that there is more cholesterol available on the limiting membrane under these conditions. Interestingly, it was suggested that caveolin in multimeric/caveolar structures has a higher affinity for cholesterol than caveolin monomers (Bauer and Pelkmans, 2006). The authors proposed an interesting model that links cholesterol sensing and/or

distribution of cholesterol among cellular membranes is crucial for normal cellular function, and it is well known that there are vesicle-independent, vesicle-dependent, and even energy-independent mechanisms for moving cholesterol from one membrane compartment to another (Hao *et al.*, 2002; Soccio and Breslow, 2004; Ikonen, 2008; Mesmin and Maxfield, 2009). It is clear from all these studies that intracellular cholesterol transport is a dynamic process that is facilitated but not absolutely dependent on any one of these pathways or proteins. Therefore, one would not expect there to be an absolute requirement for caveolin-1 to transport cholesterol. The challenge for the future is to determine the mechanism underlying caveolin-1 movements to and from different intracellular compartments and the machinery that regulates this process.

MATERIALS AND METHODS

Cell lines, transfection, and protein labeling

The stably transfected CHO cell line used in these experiments was characterized and described previously (Mundy *et al.*, 2002). Cells were grown in DMEM (Invitrogen, Carlsbad, CA) supplemented with 10% fetal calf serum (FCS) and 40 µg/ml proline in a humidified CO₂ (5%) incubator at 37°C. Primary human fibroblasts and SV589, a human fibroblast cell line, were grown as previously described (Goldstein *et al.*, 1983). Starvation of cells was generally done overnight by replacing the growth medium with DMEM containing proline for CHO cells but no FCS. Normal human fibroblasts were starved in DMEM without added FCS. Cells were imaged either 24 or 48 h later. SV589 cells were transfected using FuGENE HD (Roche Diagnostics, Indianapolis, IN). Briefly, 2 µg of DNA was used per 35-mm dish with 6 µl of FuGENE HD following the manufacturer's instructions. Cells were imaged 24–48 h after transfection.

To assess protein turnover, the stable cell line was labeled for 2 h with 0.2 mCi/ml of EasyTag EXPRESS^{35S} Protein Labeling Mix (PerkinElmer, Waltham, MA) in Cys/Met-free medium (Sigma-Aldrich, St. Louis, MO), chased for 30 min in growth medium, and further chased for the indicated times in growth medium, starvation medium, or growth medium containing 2.5 µg/ml U18666A. At each time point the cells were harvested and solubilized in immunoprecipitation (IP) buffer (25 mM Tris-HCl, pH 7.5, 5 mM EDTA, 150 mM NaCl, 1% Triton X-100, 60 mM octylglucoside with protease inhibitors), and caveolin (both endogenous and caveolin-1-GFP) was immunoprecipitated overnight with 2 µg of a polyclonal anti-caveolin antibody (Transduction Labs/BD Biosciences, Franklin Lakes, NJ). Immunoprecipitates were collected using protein A-Sepharose (GE Healthcare, Piscataway, NJ), washed with IP buffer, and separated by SDS-PAGE. The labeled proteins were visualized on a phosphorimager (Typhoon Trio, GE Healthcare), and the bands were quantified using ImageJ (National Institutes of Health, Bethesda, MD).

Live-cell imaging and immunofluorescence microscopy

Cells for live-cell imaging were grown and maintained in 35-mm glass-bottomed dishes (MatTek, Ashland, MA), and the dishes were placed in a humidified chamber and maintained at 37°C and 5% CO₂ throughout the experiment. Cells were imaged using a Leica (Wetzlar, Germany) TCS-SP laser scanning confocal microscope with a 100×, 1.4 numerical aperture (NA), plan Apochromatic lens using a computer-controlled 488-nm argon laser to excite GFP or a 568-nm krypton laser to excite Alexa red dyes coupled to dextran and LysoTracker (Invitrogen Molecular Probes, Eugene, OR). Signals were collected at 1.3-s intervals. FRAP was performed as

described (Mundy *et al.*, 2002). Some live-cell imaging was done on a DeltaVision deconvolution microscope (Applied Precision, Issaquah, WA) using a 100×, 1.4 NA lens. Acquisition rates for time lapse varied from 1 to 1.6 frames per second.

The lysosomal fluorescence intensity was determined from summed deconvolved slices from 10 to 12 cells each in four separate experiments. The lysosomal areas were outlined using ImageJ and an integrated fluorescence intensity from that region determined. We then subtracted the contribution of the top plus bottom by measuring an area that contained no lysosomes and then outlined the entire cell to obtain the percentage of the total fluorescence on lysosomes. The graphs in Figure 4D were generated by drawing a line along the edge of the cell in both the starved and the reversed image using the freehand line tool of ImageJ, and a line profile was generated using the Plot Profile function. The peaks represent the amount of fluorescence in each spot and are expressed as gray values (arbitrary units). To quantify the amount of caveolin at the plasma membrane after reversal, 10 random areas were selected using the point visiting function of a DeltaVision deconvolution microscope, and a complete stack was taken either before or 15 min after reversal with fresh growth medium. The individual stacked images were summed and corrected for photobleaching, and 38 areas were selected (at least three to four from each of the 10 fields) that contained individual cells with edges that did not overlap with other cells. The mean fluorescence intensity was measured and the ratios determined from the reversed image divided by the before image. The ratio was 1.43 ± 0.04 (SEM).

To determine the colocalization of caveolin-1-GFP and LysoTracker, we used the Coloc module of Imaris software, version 5.5.2 (Bitplane, St. Paul, MN). The source images were first thresholded so the background was zero, and the data set was masked using the red channel (LysoTracker). The program was then allowed to automatically find the channel intensity thresholds above which colocalization was statistically significant, and Pearson's *r* was determined.

For staining of LE/lysosomes with antibodies, human fibroblasts were fixed and permeabilized with -20°C methanol for 5 min, blocked with 0.2% fish skin gelatin, and labeled with an anti-LAMP-1 antibody (Santa Cruz Biotechnology, Santa Cruz, CA). A secondary antibody conjugated to Alexa 568 dye (Invitrogen Molecular Probes) was used to visualize the primary antibody. Filipin staining was performed as described (Blanchette-Mackie *et al.*, 1989), and images were acquired on a DeltaVision deconvolution microscope using a 4',6'-diamidino-2-phenylindole (DAPI) filter set.

Immunogold labeling and electron microscopy

Cells were labeled and processed for electron microscopy essentially as described (Roth, 1989; del Pozo *et al.*, 2005). Briefly, cells were fixed in 3% (wt/vol) formaldehyde/0.1% glutaraldehyde in warm Hank's balanced salt solution-4-(2-hydroxyethyl)-1-piperazineethanesulfonic acid (HEPES; 20 mM, pH 7.3) for 1 h and quenched in 50 mM ammonium chloride in phosphate-buffered saline (PBS) for 30 min. Cell pellets were embedded in Lowicryl K4M at -35°C, and the Lowicryl resin was polymerized by indirect diffuse UV irradiation. For immunolabeling, sections were blocked with PBS containing 1% bovine serum albumin, 0.01% Triton X-100, and 0.01% Tween 20 and incubated for 17 h at 4°C with rabbit antiserum raised against caveolin-1 (10 µg/ml; Transduction Labs/BD Biosciences) or GFP (5 µg/ml; Clontech, Mountain View, CA) in blocking buffer. The bound primary antibody on the samples was detected with goat anti-rabbit IgG conjugated to 10-nm gold particles (1:40 dilution; Amersham/GE, Piscataway, NJ). After labeling, Lowicryl

K4M sections were rinsed with PBS and contrasted with uranyl acetate and lead acetate. Electron micrographs were taken with a JEOL 1200 electron microscope (JEOL, Peabody, MA) operating at 80 kV. For quantification at least 20–40 electron micrographs were taken randomly from each group labeled with immunogold. The number of gold particles associated with each of three regions—caveolae, lysosomes, and plasma membrane—were counted under blind conditions and expressed as the number of gold particles per micrometer length of the individual membranes. See Supplemental Table S1 for details of number of cells and length of membrane analyzed for each region. Gold particles were detected decorating mostly the periphery of LE/lysosomes and were scored as being associated with the periphery if they were within 20 nm of the outer surface.

Measurement of LE/lysosomal pH in live cells using ratiometric fluorescence microscopy

LE/lysosomes were labeled by endocytosis of fluorescently tagged dextrans with an average molecular weight of 10,000 Da. CHO cells were labeled overnight at 37°C with 0.3–1 mg/ml FITC-dex and 0.3 mg/ml OG-dex in either growth or starvation medium. All dextrans were obtained from Invitrogen Molecular Probes. The labeling medium was then removed, and cells were chased for ≥ 2 h before imaging. Fluorescence images of labeled cells were collected using a PerkinElmer UltraView ERS spinning disk confocal microscope at an emission wavelength of 510 nm with excitation at 440 and 488 nm. The pH of the labeled organelles was determined from the FITC-dex and OG-dex fluorescence ratios (488/440 ratios), essentially as described (Christensen *et al.*, 2002), by comparison to standard curves generated for each experiment.

All images were processed using the open-source software ImageJ. To obtain an organelle pH ratio, the signal from the background-subtracted 488-nm image was divided by the signal from the background-subtracted 440-nm image to obtain a ratio image. Next a binary mask was generated from the 488-nm image by adjusting the intensity threshold to include only the labeled organelles. By overlaying the binary mask on the ratio image, measurements of ratios were restricted to the organelles of interest. These were then exported to Excel (Microsoft, Redmond, WA) for further data processing and analysis.

A second method was used to measure LE/lysosomal pH and was based again on the ratio of pH-sensitive FITC fluorescence to a pH-insensitive dye, rhodamine (Majumdar *et al.*, 2007). In this case, cells were loaded with a 70,000-Da dextran that was coupled to both FITC and rhodamine (FITC/RH-dex) at 1 mg/ml overnight in either growth medium or starvation medium. The cells were then chased as described in the respective growth or starvation medium without any labeled dextran before imaging using excitation wavelengths of 488 for FITC and 568 for rhodamine. Emissions were collected using a 527(55) bandpass filter for FITC and a 615(70) bandpass filter for rhodamine. The images were processed using Image J essentially as described, using the 527/615 emission ratio. The averages of the ratios from ~2000–4000 lysosomes were converted to pH values by comparison with a standard curve determined by clamping the pH using the approach described by Christensen *et al.* (2002) (Supplemental Figure S3A). To clamp LE/lysosome pH, dye-labeled cells were equilibrated for 10 min in calibration buffer (130 mM KCl, 1 mM MgCl₂, 15 mM HEPES, 15 mM 2-(*N*-morpholino)ethanesulfonic acid, pH 7) that contained 10 μ M of the H⁺ ionophore nigericin and 10 μ M of the K⁺ ionophore valinomycin. Images were collected as indicated, and the buffer was replaced with fresh calibration buffer at pH 6.5; after 10 min, images were again collected. This process was repeated at pH 6.0, 5.5, 5.0, 4.5, and 4.0.

The average intensity ratios from ~2000–4000 labeled organelles were plotted against pH and gave a nearly linear response between pH 4.5 and 7. The points were fit using linear regression analysis and used to convert the experimentally determined ratios to pH values. Between three and six images were used to collect data for each determination.

ACKNOWLEDGMENTS

We thank Joachim Seemann and Peter Michaely for critical reading of the manuscript. We acknowledge the UT Southwestern Live Cell Imaging Core Facility (Dallas, TX) for the use and maintenance of the microscopes. We also thank Jason Hall for his invaluable technical expertise. This work was supported by an Advance Fellow Grant from the National Science Foundation to D.M. and National Institutes of Health Grants HL 20948 and GM 52016, the Perot Family Foundation, and the Cecil H. Green Distinguished Chair in Cellular and Molecular Biology (UT Southwestern Medical Center) to R.G.W.A. This article is dedicated to the memory of Richard Anderson, a great friend, mentor, and colleague.

REFERENCES

- Abi-Mosleh L, Infante RE, Radhakrishnan A, Goldstein JL, Brown MS (2009). Cyclodextrin overcomes deficient lysosome-to-endoplasmic reticulum transport of cholesterol in Niemann-Pick type C cells. *Proc Natl Acad Sci USA* 106, 19316–19321.
- Aboulaich N, Vainonen JP, Stralfors P, Vener AV (2004). Vectorial proteomics reveal targeting, phosphorylation and specific fragmentation of polymerase I and transcript release factor (PTRF) at the surface of caveolae in human adipocytes. *Biochem J* 383, 237–248.
- Babalola JO, Wendeler M, Breiden B, Arentz C, Schwarzmann G, Locatelli-Hoops S, Sandhoff K (2007). Development of an assay for the intermembrane transfer of cholesterol by Niemann-Pick C2 protein. *Biol Chem* 388, 617–626.
- Bauer M, Pelkmans L (2006). A new paradigm for membrane-organizing and -shaping scaffolds. *FEBS Lett* 580, 5559–5564.
- Bayer N, Schober D, Prchla E, Murphy RF, Blaas D, Fuchs R (1998). Effect of bafilomycin A1 and nocodazole on endocytic transport in HeLa cells: implications for viral uncoating and infection. *J Virol* 72, 9645–9655.
- Blanchette-Mackie EJ, Dwyer NK, Amende LA (1989). Cytochemical studies of lipid metabolism: immunogold probes for lipoprotein lipase and cholesterol. *Am J Anat* 185, 255–263.
- Bosch M *et al.* (2011). Caveolin-1 deficiency causes cholesterol-dependent mitochondrial dysfunction and apoptotic susceptibility. *Curr Biol* 21, 681–686.
- Boucrot E, Howes MT, Kirchhausen T, Parton RG (2011). Redistribution of caveolae during mitosis. *J Cell Sci* 124, 1965–1972.
- Bright NA, Gratian MJ, Luzio JP (2005). Endocytic delivery to lysosomes mediated by concurrent fusion and kissing events in living cells. *Curr Biol* 15, 360–365.
- Brown MS, Goldstein JL (1986). A receptor-mediated pathway for cholesterol homeostasis. *Science* 232, 34–47.
- Butler JD *et al.* (1992). Progesterone blocks cholesterol translocation from lysosomes. *J Biol Chem* 267, 23797–23805.
- Cenedella RJ (2009). Cholesterol synthesis inhibitor U18666A and the role of sterol metabolism and trafficking in numerous pathophysiological processes. *Lipids* 44, 477–487.
- Chen JW, Murphy TL, Willingham MC, Pastan I, August JT (1985). Identification of two lysosomal membrane glycoproteins. *J Cell Biol* 101, 85–95.
- Cheng ZJ, Singh RD, Marks DL, Pagano RE (2006a). Membrane microdomains, caveolae, and caveolar endocytosis of sphingolipids. *Mol Membrane Biol* 23, 101–110.
- Cheng ZJ, Singh RD, Sharma DK, Holicky EL, Hanada K, Marks DL, Pagano RE (2006b). Distinct mechanisms of clathrin-independent endocytosis have unique sphingolipid requirements. *Mol Biol Cell* 17, 3197–3210.
- Cheruku SR, Xu Z, Dutia R, Lobel P, Storch J (2006). Mechanism of cholesterol transfer from the Niemann-Pick type C2 protein to model membranes supports a role in lysosomal cholesterol transport. *J Biol Chem* 281, 31594–31604.
- Christensen KA, Myers JT, Swanson JA (2002). pH-dependent regulation of lysosomal calcium in macrophages. *J Cell Sci* 115, 599–607.

- Damm EM, Pelkmans L, Kartenbeck J, Mezzacasa A, Kurzchalia T, Helenius A (2005). Clathrin- and caveolin-1-independent endocytosis: entry of simian virus 40 into cells devoid of caveolae. *J Cell Biol* 168, 477–488.
- de Brito OM, Scorrano L (2008). Mitofusin 2 tethers endoplasmic reticulum to mitochondria. *Nature* 456, 605–610.
- del Pozo MA, Balasubramanian N, Alderson NB, Kiosses WB, Grande-Garcia A, Anderson RG, Schwartz MA (2005). Phospho-caveolin-1 mediates integrin-regulated membrane domain internalization. *Nat Cell Biol* 7, 901–908.
- Drab M *et al.* (2001). Loss of caveolae, vascular dysfunction, and pulmonary defects in caveolin-1 gene-disrupted mice. *Science* 293, 2449–2452.
- Dupree P, Parton RG, Raposo G, Kurzchalia TV, Simons K (1993). Caveolae and sorting in the trans-Golgi network of epithelial cells. *EMBO J* 12, 1597–1605.
- Fielding PE, Chau P, Liu D, Spencer TA, Fielding CJ (2004). Mechanism of platelet-derived growth factor-dependent caveolin-1 phosphorylation: relationship to sterol binding and the role of serine-80. *Biochem J* 43, 2578–2586.
- Fielding PE, Fielding CJ (1995). Plasma membrane caveolae mediate the efflux of cellular free cholesterol. *Biochem J* 314, 14288–14292.
- Frank PG, Cheung MW, Pavlides S, Llaveras G, Park DS, Lisanti MP (2006). Caveolin-1 and regulation of cellular cholesterol homeostasis. *Am J Physiol* 291, H677–H686.
- Fu Y, Hoang A, Escher G, Parton RG, Krozowski Z, Sviridov D (2004). Expression of caveolin-1 enhances cholesterol efflux in hepatic cells. *J Biol Chem* 279, 14140–14146.
- Furuchi T, Aikawa K, Arai H, Inoue K (1993). Bafilomycin A1, a specific inhibitor of vacuolar-type H(+)-ATPase, blocks lysosomal cholesterol trafficking in macrophages. *J Biol Chem* 268, 27345–27348.
- Goldstein JL, Basu SK, Brown MS (1983). Receptor-mediated endocytosis of low-density lipoprotein in cultured cells. *Methods Enzymol* 98, 241–260.
- Hansen CG, Bright NA, Howard G, Nichols BJ (2009). SDPR induces membrane curvature and functions in the formation of caveolae. *Nat Cell Biol* 11, 807–814.
- Hao M, Lin SX, Karylowski OJ, Wustner D, McGraw TE, Maxfield FR (2002). Vesicular and non-vesicular sterol transport in living cells. The endocytic recycling compartment is a major sterol storage organelle. *J Biol Chem* 277, 609–617.
- Hayer A, Stoeber M, Ritz D, Engel S, Meyer HH, Helenius A (2010). Caveolin-1 is ubiquitinated and targeted to intraluminal vesicles in endolysosomes for degradation. *J Cell Biol* 191, 615–629.
- Hill MM *et al.* (2008). PTRF-cavin, a conserved cytoplasmic protein required for caveola formation and function. *Cell* 132, 113–124.
- Ikonen E (2008). Cellular cholesterol trafficking and compartmentalization. *Nat Rev* 9, 125–138.
- Ikonen E, Parton RG (2000). Caveolins and cellular cholesterol balance. *Traffic* 1, 212–217.
- Infante RE, Wang ML, Radhakrishnan A, Kwon HJ, Brown MS, Goldstein JL (2008). NPC2 facilitates bidirectional transfer of cholesterol between NPC1 and lipid bilayers, a step in cholesterol egress from lysosomes. *Proc Natl Acad Sci USA* 105, 15287–15292.
- Karjalainen M, Kakkonen E, Upla P, Paloranta H, Kankaanpaa P, Liberali P, Renkema GH, Hyypia T, Heino J, Marjomaki V (2008). A Raft-derived, Pak1-regulated entry participates in alpha2beta1 integrin-dependent sorting to caveosomes. *Mol Biol Cell* 19, 2857–2869.
- Kirkham M, Fujita A, Chadda R, Nixon SJ, Kurzchalia TV, Sharma DK, Pagano RE, Hancock JF, Mayor S, Parton RG (2005). Ultrastructural identification of uncoated caveolin-independent early endocytic vehicles. *J Cell Biol* 168, 465–476.
- Koster JF, Vaandrager H, van Berkel TJ (1980). Study of the hydrolysis of 4-methylumbelliferyl oleate by acid lipase and cholesteryl oleate by acid cholesteryl esterase in human leucocytes, fibroblasts and liver. *Biochim Biophys Acta* 618, 98–105.
- Le PU, Guay G, Altschuler Y, Nabi IR (2002). Caveolin-1 is a negative regulator of caveolae-mediated endocytosis to the endoplasmic reticulum. *J Biol Chem* 277, 3371–3379.
- Le Lay S, Hajdich E, Lindsay MR, Le Liepvre X, Thiele C, Ferre P, Parton RG, Kurzchalia T, Simons K, Dugail I (2006). Cholesterol-induced caveolin targeting to lipid droplets in adipocytes: a role for caveolar endocytosis. *Traffic* 7, 549–561.
- Li Y, Wandinger-Ness A, Goldenring JR, Cover TL (2004). Clustering and redistribution of late endocytic compartments in response to *Helicobacter pylori* vacuolating toxin. *Mol Biol Cell* 15, 1946–1959.
- Liscum L, Sturley SL (2004). Intracellular trafficking of Niemann-Pick C proteins 1 and 2: obligate components of subcellular lipid transport. *Biochim Biophys Acta* 1685, 22–27.
- Liu CH, Thangada S, Lee MJ, Van Brocklyn JR, Spiegel S, Hla T (1999). Ligand-induced trafficking of the sphingosine-1-phosphate receptor EDG-1. *Mol Biol Cell* 10, 1179–1190.
- Liu L, Pilch PF (2008). A critical role of cavin (polymerase I and transcript release factor) in caveolae formation and organization. *J Biol Chem* 283, 4314–4322.
- Majumdar A, Cruz D, Asamoah N, Buxbaum A, Sohar I, Lobel P, Maxfield FR (2007). Activation of microglia acidifies lysosomes and leads to degradation of Alzheimer amyloid fibrils. *Mol Biol Cell* 18, 1490–1496.
- Marsh M, Wellsted J, Kern H, Harms E, Helenius A (1982). Monensin inhibits Semliki Forest virus penetration into culture cells. *Proc Natl Acad Sci USA* 79, 5297–5301.
- Martin S, Parton RG (2005). Caveolin, cholesterol, and lipid bodies. *Semin Cell Dev Biol* 16, 163–174.
- McGookey DJ, Anderson RG (1983). Morphological characterization of the cholesteryl ester cycle in cultured mouse macrophage foam cells. *J Cell Biol* 97, 1156–1168.
- McMahon KA, Zajicek H, Li WP, Peyton MJ, Minna JD, Hernandez VJ, Luby-Phelps K, Anderson RG (2009). SRBC/cavin-3 is a caveolin adapter protein that regulates caveolae function. *EMBO J* 28, 1001–1015.
- Mesa R, Salomon C, Roggero M, Stahl PD, Mayorga LS (2001). Rab22a affects the morphology and function of the endocytic pathway. *J Cell Sci* 114, 4041–4049.
- Mesmin B, Maxfield FR (2009). Intracellular sterol dynamics. *Biochim Biophys Acta* 1791, 636–645.
- Mundy DI, Machleidt T, Ying YS, Anderson RG, Bloom GS (2002). Dual control of caveolar membrane traffic by microtubules and the actin cytoskeleton. *J Cell Sci* 115, 4327–4339.
- Murata M, Peranen J, Schreiner R, Wieland F, Kurzchalia TV, Simons K (1995). VIP21/caveolin is a cholesterol-binding protein. *Proc Natl Acad Sci USA* 92, 10339–10343.
- Parpal S, Karlsson M, Thorn H, Stralfors P (2001). Cholesterol depletion disrupts caveolae and insulin receptor signaling for metabolic control via insulin receptor substrate-1, but not for mitogen-activated protein kinase control. *J Biol Chem* 276, 9670–9678.
- Parton RG, Hanzal-Bayer M, Hancock JF (2006). Biogenesis of caveolae: a structural model for caveolin-induced domain formation. *J Cell Sci* 119, 787–796.
- Parton RG, Joggerst B, Simons K (1994). Regulated internalization of caveolae. *J Cell Biol* 127, 1199–1215.
- Parton RG, Simons K (2007). The multiple faces of caveolae. *Nat Rev* 8, 185–194.
- Patterson GH, Knobel SM, Sharif WD, Kain SR, Piston DW (1997). Use of the green fluorescent protein and its mutants in quantitative fluorescence microscopy. *Biophys J* 73, 2782–2790.
- Pelkmans L (2005). Secrets of caveolae- and lipid raft-mediated endocytosis revealed by mammalian viruses. *Biochim Biophys Acta* 1746, 295–304.
- Pelkmans L, Burli T, Zerial M, Helenius A (2004). Caveolin-stabilized membrane domains as multifunctional transport and sorting devices in endocytic membrane traffic. *Cell* 118, 767–780.
- Pelkmans L, Kartenbeck J, Helenius A (2001). Caveolar endocytosis of simian virus 40 reveals a new two-step vesicular-transport pathway to the ER. *Nat Cell Biol* 3, 473–483.
- Pelkmans L, Puntener D, Helenius A (2002). Local actin polymerization and dynamin recruitment in SV40-induced internalization of caveolae. *Science* 296, 535–539.
- Pelkmans L, Zerial M (2005). Kinase-regulated quantal assemblies and kiss-and-run recycling of caveolae. *Nature* 436, 128–133.
- Pichler H, Gaigg B, Hrastnik C, Achleitner G, Kohlwein SD, Zellnig G, Perktold A, Daum G (2001). A subfraction of the yeast endoplasmic reticulum associates with the plasma membrane and has a high capacity to synthesize lipids. *Eur J Biochem* 268, 2351–2361.
- Pietiainen V, Marjomaki V, Upla P, Pelkmans L, Helenius A, Hyypia T (2004). Echovirus 1 endocytosis into caveosomes requires lipid rafts, dynamin II, and signaling events. *Mol Biol Cell* 15, 4911–4925.
- Pol A, Luetterforst R, Lindsay M, Heino S, Ikonen E, Parton RG (2001). A caveolin dominant negative mutant associates with lipid bodies and induces intracellular cholesterol imbalance. *J Cell Biol* 152, 1057–1070.
- Pol A, Martin S, Fernandez MA, Ingelmo-Torres M, Ferguson C, Enrich C, Parton RG (2005). Cholesterol and fatty acids regulate dynamic caveolin trafficking through the Golgi complex and between the cell surface and lipid bodies. *Mol Biol Cell* 16, 2091–2105.
- Rodal SK, Skretting F, Garred O, Vilhardt F, van Deurs B, Sandvig K (1999). Extraction of cholesterol with methyl-beta-cyclodextrin perturbs formation of clathrin-coated endocytic vesicles. *Mol Biol Cell* 10, 961–974.

- Rohrer J, Schweizer A, Russell D, Kornfeld S (1996). The targeting of Lamp1 to lysosomes is dependent on the spacing of its cytoplasmic tail tyrosine sorting motif relative to the membrane. *J Cell Biol* 132, 565–576.
- Rosenbaum AI, Zhang G, Warren JD, Maxfield FR (2010). Endocytosis of beta-cyclodextrins is responsible for cholesterol reduction in Niemann-Pick type C mutant cells. *Proc Natl Acad Sci USA* 107, 5477–5482.
- Roth J (1989). Postembedding labeling on Lowicryl K4M tissue sections: detection and modification of cellular components. *Methods Cell Biol* 31, 513–551.
- Rothberg KG, Heuser JE, Donzell WC, Ying YS, Glenney JR, Anderson RG (1992). Caveolin, a protein component of caveolae membrane coats. *Cell* 68, 673–682.
- Roy S, Luetterforst R, Harding A, Apolloni A, Etheridge M, Stang E, Rolls B, Hancock JF, Parton RG (1999). Dominant-negative caveolin inhibits H-Ras function by disrupting cholesterol-rich plasma membrane domains. *Nat Cell Biol* 1, 98–105.
- Sharma DK, Brown JC, Choudhury A, Peterson TE, Holicky E, Marks DL, Simari R, Parton RG, Pagano RE (2004). Selective stimulation of caveolar endocytosis by glycosphingolipids and cholesterol. *Mol Biol Cell* 15, 3114–3122.
- Simionescu N (1983). Cellular aspects of transcapillary exchange. *Physiol Rev* 63, 1536–1579.
- Singh RD, Puri V, Valiyaveetil JT, Marks DL, Bittman R, Pagano RE (2003). Selective caveolin-1-dependent endocytosis of glycosphingolipids. *Mol Biol Cell* 14, 3254–3265.
- Smart EJ, Ying Y, Donzell WC, Anderson RG (1996). A role for caveolin in transport of cholesterol from endoplasmic reticulum to plasma membrane. *J Biol Chem* 271, 29427–29435.
- Soccio RE, Breslow JL (2004). Intracellular cholesterol transport. *Arterioscler Thromb Vasc Biol* 24, 1150–1160.
- Tagawa A, Mezzacasa A, Hayer A, Longatti A, Pelkmans L, Helenius A (2005). Assembly and trafficking of caveolar domains in the cell: caveolae as stable, cargo-triggered, vesicular transporters. *J Cell Biol* 170, 769–779.
- Thiele C, Hannah MJ, Fahrenholz F, Huttner WB (2000). Cholesterol binds to synaptophysin and is required for biogenesis of synaptic vesicles. *Nat Cell Biol* 2, 42–49.
- Trigatti BL, Anderson RG, Gerber GE (1999). Identification of caveolin-1 as a fatty acid binding protein. *Biochem Biophys Res Commun* 255, 34–39.
- Verma P, Ostermeyer-Fay AG, Brown DA (2010). Caveolin-1 induces formation of membrane tubules that sense actomyosin tension and are inhibited by polymerase I and transcript release factor/cavin-1. *Mol Biol Cell* 21, 2226–2240.
- Vinten J, Voldstedlund M, Clausen H, Christiansen K, Carlsen J, Tranum-Jensen J (2001). A 60-kDa protein abundant in adipocyte caveolae. *Cell Tissue Res* 305, 99–106.
- Voelker DR (2003). New perspectives on the regulation of intermembrane glycerophospholipid traffic. *J Lipid Res* 44, 441–449.
- Voeltz GK, Prinz WA (2007). Sheets, ribbons and tubules—how organelles get their shape. *Nat Rev* 8, 258–264.
- Voldstedlund M, Vinten J, Tranum-Jensen J (2001). cav-p60 expression in rat muscle tissues. Distribution of caveolar proteins. *Cell Tissue Res* 306, 265–276.
- Wileman T, Boshans RL, Schlesinger P, Stahl P (1984). Monensin inhibits recycling of macrophage mannose-glycoprotein receptors and ligand delivery to lysosomes. *Biochem J* 220, 665–675.
- Williams TM, Lisanti MP (2004). The caveolin genes: from cell biology to medicine. *Ann Med* 36, 584–595.
- Yoshimori T, Yamamoto A, Moriyama Y, Futai M, Tashiro Y (1991). Bafilomycin A1, a specific inhibitor of vacuolar-type H(+)-ATPase, inhibits acidification and protein degradation in lysosomes of cultured cells. *J Biol Chem* 266, 17707–17712.